HYDROGEN MASER ADVANCED DEVELOPMENT
ATOMIC HYDROGEN FREQUENCY STANDARD

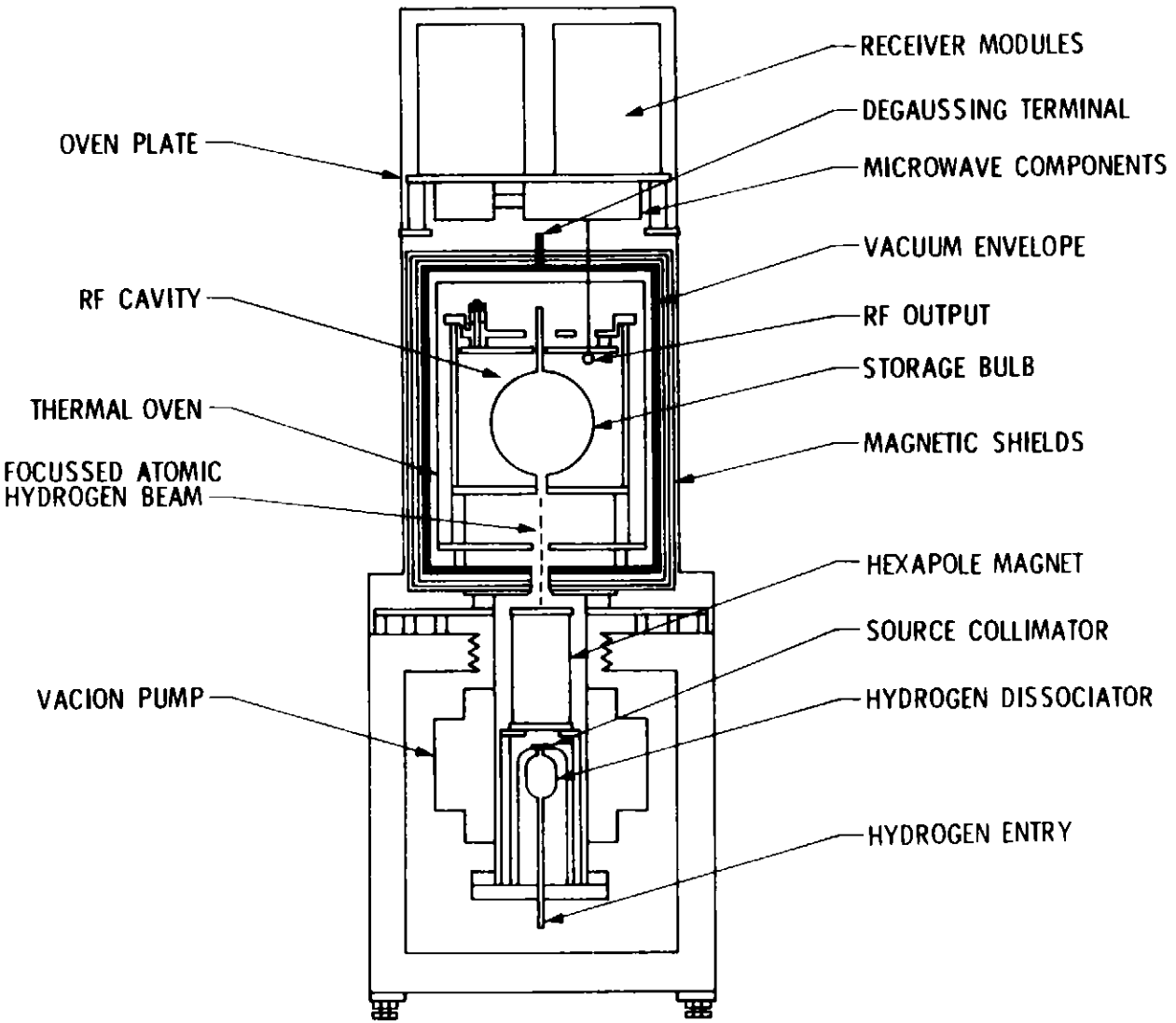

AT 14.4/001

Presented at 14th Annual
Precise Time and Time Interval
(PTTI) Applications and Planning
Meeting on 12/1/82

EVALUATION OF MODERN HYDROGEN MASERS*

Albert Kirk, Paul Kuhnle and Richard Sydnor
Jet Propulsion Laboratory
California Institute of Technology
Pasadena, California

ABSTRACT

During the last two years the Jet Propulsion Laboratory (JPL) has been conducting an evaluation of modern hydrogen masers in a program sponsored by the National Aeronautics and Space Administration (NASA). The goal was to perform a series of tests and evaluations which would be as complete, accurate and unbiased as possible. A board of nationally recognized experts in hydrogen masers and in frequency and time was selected to design the testing program, supervise the tests and release the final report. This board consisted of:

Hugh Fosque	NASA Headquarters	Chairman
Joel Smith	JPL	Convening Authority
Norman Ramsey	Harvard University	
Robert Vessot	Smithsonian Astrophysical Observatory (SAO)	
Victor Reinhardt	Goddard Space Flight Center (GSFC)	
Richard Sydnor	JPL	
James Barnes	National Bureau of Standards, Boulder (NBS)	
Gernot Winkler	United States Naval Observatory (USNO)	
Andrew Chi	GSFC	
Arthur Zygielbaum	JPL	Executive Secretary

The maser types tested were the SAO VLG-11B, the GSFC NR and, as a result of the testing process, the JPL DSN. The masers were tested for environmental sensitivities (magnetic field, temperature, barometric pressure) and long-term aging. Allan variance runs of 72 days were made in order to attain averaging times from several seconds to 10^6 seconds. Auto- and cross-correlation techniques were used to determine the effects of uncontrolled parameters such as humidity. Three-cornered-hat and other data reduction techniques were used to determine the characteristics of the individual masers.

*The research described in this paper was carried out by the Jet Propulsion Laboratory, California Institute of Technology, under contract with the National Aeronautics and Space Administration.

(2) I.F. Meter Calibration

To allow correct interpretation of the data that was collected, certain conditions must be stated. Maser cavity output power is one of those. Since output power of a maser is normally indicated on a front panel display, which is derived from an I.F. power measurement, the display is calibrated with reference to the actual maser cavity output power by substituting a precisely known signal for that of the cavity output. The resulting calibration charts are shown in Figures 1 and 2.

(3) Pressure Control Setting Dependent Parameters

The operating point of a maser is a function of the hydrogen gas pressure setting. Output power, line Q, vacion current and hydrogen source dissociator efficiency are determined by this setting. All these variables were recorded for different pressure control settings and the data subsequently graphed. Of particular interest is the relationship of line Q vs. output power. Knowledge of this data is essential for diagnostic purposes. This "baseline" data was also used to determine the optimal operating conditions of each maser for all subsequent tests. The measurement results are shown in Figures 3, 4, 5 and 6.

(4) Environmental Tests

a. Output Frequency Vs. Input Voltage

The DC input voltage was stepped between 22 and 31V while the output frequency was monitored. Sufficient time was allowed between each voltage step for the maser frequency to shift and settle. This test sequence was repeated several times. The NR-4 showed no measurable frequency shift above the recorded noise level of 1×10^{-14}.

The SAO-14 indicated variations on the order of 5×10^{-15}. This value is at the level of the measurement uncertainty. The results shown are for the entire 22 to 31 VDC test range. Figure 7 shows the output frequency variations of NR-4 and a reference maser during the above test sequence.

b. Output Frequency Vs. Ambient Magnetic Field

A 90-inch diameter helmholtz coil was placed about the hydrogen maser under test to produce a DC magnetic field aligned with the maser's vertical axis. Initial testing was done by varying the magnetic field in small steps first in one direction up to a specified maximum value then back to zero and then continuing in small steps in the opposite direction up to the specified maximum value and again back to zero. Thus the test went around the "loop" once. Output frequency, Zeeman frequency and output power were measured and recorded at each step as shown in Figure 8. This test is difficult to perform since any overshoot in field variations causes hysteresis distortion. Repeatability was poor. It does however show the effects of hysteresis and the fact that the slope is influenced by the way the test is done.

e. Output Frequency Vs. Time

The output frequency of a hydrogen maser at any given time depends on its random behavior, its susceptibility to the environment and its aging mechanism. Random behavior as a function of measurement time can be predicted. A statistical technique of measuring this behavior is known as the Allan Variance which results in a sigma/tau plot of frequency stability vs. measurement time.[1] This type of measurement was performed and will be discussed in the following section. It should be clearly understood however that when the systematic effects of the environment and aging on a masers output frequency dominate over its random behavior, which is usually the case for measurement times greater than a few thousand seconds, the Allan Variance plot ceases to convey random behavior and must be interpreted carefully. There are methods of removing long term drift but the degree of success depends on precise knowledge of this drift. The method we used to determine long term behavior of output frequency vs. time was to manually spin exchange tune the masers periodically and plot the resulting maser cavity frequency as a function of time. This was combined with measuring the relative frequency offset of the various masers involved at the time they were tuned to separate output frequency changes due to cavity aging from other effects. The resulting data clearly shows that cavity aging can be significant.

Figure 15 is a plot of cavity frequency vs. time for NR-4 over a 500 day period. The ordinate scale of the graph is the cavity register bit setting required for the maser to be tuned. Each dot represents a tuning event. We assumed the cavity Q to be constant. The line Q was periodically measured and found to be constant for a given operating point. Between days 200 and 500 the $\Delta fo/_f$/cavity bit = 1.166×10^{-16}. The output frequency aging rate due to cavity pulling for this maser was thus determined to be -1.35×10^{-14}/day at a hydrogen flux pressure control setting of 450 and a hydrogen line Q of 1.64×10^9. The frequency offset change near day 50 was probably due to mechanical shock since work was done on the maser during that period. Between 10-22-81 and 1-1-82 the masers output frequency was monitored continuously against 3 other masers and no sudden shifts in output frequency between NR-4 and the reference masers was found. Furthermore, Figure 15 data suggests that the cavity shifted more than expected during that period by about 3000 bits. Actual output frequency measurements however indicated that less of a frequency change took place. A possible explanation is that the atomic operating frequency increased by 3.5×10^{-13} during that period. A Zeeman frequency measurement showed no significant change.

Figure 16 is a plot of cavity frequency vs. time for SAO-14 covering an 800 day period. The ordinate scale of the graph is the cavity tuning varactor diode bias voltage setting required for the maser to be tuned. D = Drift per day and was calculated for consecutive time segments assuming a line Q of 1.84×10^9 and corrected for diode nonlinearity. The value of D is inversely proportional to operating point line Q. The large shifts shown on days 100, 150, 375 are due to experimental work that was performed with the cavity RF probe output coax cable. Unlike the NR-4 maser the cavity frequency of SAO-14 changed at a fairly high rate when the maser was new but

(2) I.F. Meter Calibration

To allow correct interpretation of the data that was collected, certain conditions must be stated. Maser cavity output power is one of those. Since output power of a maser is normally indicated on a front panel display, which is derived from an I.F. power measurement, the display is calibrated with reference to the actual maser cavity output power by substituting a precisely known signal for that of the cavity output. The resulting calibration charts are shown in Figures 1 and 2.

(3) Pressure Control Setting Dependent Parameters

The operating point of a maser is a function of the hydrogen gas pressure setting. Output power, line Q, vacion current and hydrogen source dissociator efficiency are determined by this setting. All these variables were recorded for different pressure control settings and the data subsequently graphed. Of particular interest is the relationship of line Q vs. output power. Knowledge of this data is essential for diagnostic purposes. This "baseline" data was also used to determine the optimal operating conditions of each maser for all subsequent tests. The measurement results are shown in Figures 3, 4, 5 and 6.

(4) Environmental Tests

a. Output Frequency Vs. Input Voltage

The DC input voltage was stepped between 22 and 31V while the output frequency was monitored. Sufficient time was allowed between each voltage step for the maser frequency to shift and settle. This test sequence was repeated several times. The NR-4 showed no measurable frequency shift above the recorded noise level of 1×10^{-14}.

The SAO-14 indicated variations on the order of 5×10^{-15}. This value is at the level of the measurement uncertainty. The results shown are for the entire 22 to 31 VDC test range. Figure 7 shows the output frequency variations of NR-4 and a reference maser during the above test sequence.

b. Output Frequency Vs. Ambient Magnetic Field

A 90-inch diameter helmholtz coil was placed about the hydrogen maser under test to produce a DC magnetic field aligned with the maser's vertical axis. Initial testing was done by varying the magnetic field in small steps first in one direction up to a specified maximum value then back to zero and then continuing in small steps in the opposite direction up to the specified maximum value and again back to zero. Thus the test went around the "loop" once. Output frequency, Zeeman frequency and output power were measured and recorded at each step as shown in Figure 8. This test is difficult to perform since any overshoot in field variations causes hysteresis distortion. Repeatability was poor. It does however show the effects of hysteresis and the fact that the slope is influenced by the way the test is done.

INTRODUCTION

The three maser types evaluated represent the newest models manufactured by the Jet Propulsion Laboratory (JPL), the Goddard Space Flight Center (GSFC) and the Smithsonian Institution Astrophysical Observatory (SAO). The characteristics that distinguish these from earlier laboratory models are: transportable for routine field operation anywhere in the world, highly reliable, well documented, ease of servicing, equipped with built in instrumentation for simplified verification of performance and diminished dependence on the operating environment.

The GSFC Hydrogen Maser is manufactured by Johns Hopkins University Applied Physics Laboratory (APL) as the model NR. GSFC and APL supplied serial number four (4), identified in this paper as NR-4. The Smithsonian Astrophysical Observatory supplied one model VLG 11B serial P14 which is identified as SAO 14. This test series was conducted in the Interim Frequency Standard Test Facility located at JPL in Pasadena, California. JPL designed and maintains two reference Hydrogen Masers in this facility. These two frequency standards are identified as DSN2 and DSN3.

A considerable amount of data was collected with the goal of assessing the current state of the art of active hydrogen maser technology and to gather information that will be used to evolve a development program for the next generation of atomic frequency standards used by NASA.

The data in this paper is a small but representative sample of all the data that was collected during the tests. An official JPL report will be published in three volumes under the heading "Hydrogen Maser Comparison Test." Volume I is an executive summary covering all aspects of the test but limited in detail and amount of data. Volume II contains detailed descriptions of all tests and a complete set of all but the raw data. Volume III consists of all raw data such as magnetic tapes, strip charts, terminal print outs and log books. Due to the bulk of Volume III data specific records should be requested by those interested.

TESTS PERFORMED

A list of this test series is shown in Table 1.

(1) Verification of Inputs, Outputs and Proper Functioning of Controls

After receiving the masers, all subsystems were checked to make sure they were functioning according to JPL's and the manufacturer's expectations. Some anomalies were found and corrected by JPL or the manufacturer. The information gained was that more thorough testing is essential prior to shipment. This operation guaranteed that all subsequent tests were done with properly operating masers and assured a fair comparison of performance with minimal interruptions.

e. Output Frequency Vs. Time

The output frequency of a hydrogen maser at any given time depends on its random behavior, its susceptibility to the environment and its aging mechanism. Random behavior as a function of measurement time can be predicted. A statistical technique of measuring this behavior is known as the Allan Variance which results in a sigma/tau plot of frequency stability vs. measurement time.[1] This type of measurement was performed and will be discussed in the following section. It should be clearly understood however that when the systematic effects of the environment and aging on a masers output frequency dominate over its random behavior, which is usually the case for measurement times greater than a few thousand seconds, the Allan Variance plot ceases to convey random behavior and must be interpreted carefully. There are methods of removing long term drift but the degree of success depends on precise knowledge of this drift. The method we used to determine long term behavior of output frequency vs. time was to manually spin exchange tune the masers periodically and plot the resulting maser cavity frequency as a function of time. This was combined with measuring the relative frequency offset of the various masers involved at the time they were tuned to separate output frequency changes due to cavity aging from other effects. The resulting data clearly shows that cavity aging can be significant.

Figure 15 is a plot of cavity frequency vs. time for NR-4 over a 500 day period. The ordinate scale of the graph is the cavity register bit setting required for the maser to be tuned. Each dot represents a tuning event. We assumed the cavity Q to be constant. The line Q was periodically measured and found to be constant for a given operating point. Between days 200 and 500 the $\Delta fo/_f$/cavity bit = 1.166×10^{-16}. The output frequency aging rate due to cavity pulling for this maser was thus determined to be -1.35×10^{-14}/day at a hydrogen flux pressure control setting of 450 and a hydrogen line Q of 1.64×10^9. The frequency offset change near day 50 was probably due to mechanical shock since work was done on the maser during that period. Between 10-22-81 and 1-1-82 the masers output frequency was monitored continuously against 3 other masers and no sudden shifts in output frequency between NR-4 and the reference masers was found. Furthermore, Figure 15 data suggests that the cavity shifted more than expected during that period by about 3000 bits. Actual output frequency measurements however indicated that less of a frequency change took place. A possible explanation is that the atomic operating frequency increased by 3.5×10^{-13} during that period. A Zeeman frequency measurement showed no significant change.

Figure 16 is a plot of cavity frequency vs. time for SAO-14 covering an 800 day period. The ordinate scale of the graph is the cavity tuning varactor diode bias voltage setting required for the maser to be tuned. D = Drift per day and was calculated for consecutive time segments assuming a line Q of 1.84×10^9 and corrected for diode nonlinearity. The value of D is inversely proportional to operating point line Q. The large shifts shown on days 100, 150, 375 are due to experimental work that was performed with the cavity RF probe output coax cable. Unlike the NR-4 maser the cavity frequency of SAO-14 changed at a fairly high rate when the maser was new but

All subsequent testing was done by stepping the magnetic field equally above and below the ambient field five times. The corresponding output frequency shifts were averaged and tabulated in Figures 9 and 10. Notice that in general the hydrogen maser output frequency is more sensitive to changes in the magnetic field when the maser is operated at a higher hydrogen flux setting and also when the ambient magnetic field is varied by smaller increments. It should be noted that the data shown is for homogeneous magnetic field variations applied to the hydrogen maser's vertical axis only.

c. Output Frequency Vs. Ambient Temperature

The maser was placed in the test chamber and two separate temperature tests were performed. For one test the maser was allowed to stabilize at approximately 23°C then the temperature was increased by 3 degrees centigrade and held within ±.1°C of the setpoint until the hydrogen maser output frequency was stable. Due to random walk and aging of the test and reference hydrogen maser, the "stable frequency" is difficult to determine over a period of several hours. Hence a minimum of five thermal time constants was allowed before the temperature was decreased by 3°C. The second test was performed in a similar manner except the temperature was stepped between 21°C and 29°C. During this test as well as all others, environmental data such as temperature, humidity, atmospheric pressure and ambient magnetic field was continually recorded. It should be noted that during the temperature test the humidity inside the test chamber varied appreciably and in correlation with temperature. Since our test chamber is not equipped to control humidity, it is difficult to separate the influence that this parameter has on the hydrogen maser output frequency. The measurement results showed a coefficient $\Delta f/f/°C$ of -7×10^{-15} for the SAO-14 and -1.4×10^{-14} for the NR-4. Temperature test results are shown in Figures 11 and 12. During this test the line Q of SAO-14 was 1.7×10^{9} and that of NR-4 was 1.65×10^{9}.

d. Output Frequency Vs. Barometric Pressure

The maser was placed in the test chamber and the temperature was held constant. Several tests were performed. The test chamber barometric pressure was varied ±12" H_2O while the hydrogen maser output frequency was monitored. What distinguished one test from another was the rate at which the (barometric) pressure was changed and the dwell time. It was generally found that for fast pressure changes (Δ24" H_2O in less than 30 minutes), the output frequency varied slightly more than for slow pressure changes (Δ24" H_2O in greater than 30 minutes). It should be noted that the frequency change was of a transient nature, that is after an initial maximum deviation the frequency tended to return towards the original value. Since the frequency changes were generally small for the ±12" H_2O pressure step, measurement uncertainty due to noise and random walk of the test and reference masers is quite significant and the uncertainty is dependent on dwell time. We found for a typical slow step that the barometric pressure coefficient $\Delta f/f/"H_g$ for the SAO-14 is $+5 \times 10^{-15} \pm 5 \times 10^{-15}$, and for the NR-4 is $+1 \times 10^{-14} \pm 5 \times 10^{-15}$. Figures 13 and 14 show some typical data recorded during the barometer pressure test.

7. Tuning Repeatability

In simplified terms, a maser is considered to be tuned when the cavity frequency is set equal to the atomic operating frequency. When the cavity frequency shifts it "pulls" the atomic line frequency to produce a maser output frequency that can be described by the following equation:

$$f_o - f_A = (f_c - f_A) \frac{Q_1}{Q_c}$$

where:

f_o is the maser output frequency

f_A is the atomic operating frequency

Q_1 and Q_c are the line Q and cavity Q of that particular maser

The tuning method which we employed consisted of measuring the change in output frequency that occurred when the masers line Q (Q_1) was changed from its normal value to an arbitrarily higher value. No change in output frequency indicates that the cavity frequency is properly set.

It can be shown that $f_e = |k \Delta f \, HL|$

where f_e is the output frequency offset due to cavity mistuning. ΔfHL is the change in output frequency due to change in line Q, and

$$k = \frac{r}{r - 1}$$

where

$$r = \frac{\text{HIGH } Q_1}{\text{LOW } Q_1}$$

For a given maser, k can be easily determined and generally remains constant. It can be seen that the resolution of ΔfHL and the value of k determine the precision to which a maser can be tuned.

The following values of k were obtainable for the masers involved in this test.

NR-4 k = 12

SAO-14 k = 5.5

DSN 2 k = 3.0

DSN 3 k = 4.8

With a measurement resolution of $\pm 5 \times 10^{-15}$ the worst case frequency offset error due to cavity mistuning of the NR4 - SAO14 maser pair is estimated to be $\pm 5 \times 10^{-15} (12 + 5.5) = 8.75 \times 10^{-14}$.

this aging or settling rate diminished steadily to about 5×10^{-15}/day in terms of output frequency near the end of the test.

5. Frequency Stability - Allan Variance

Figures 17 and 18 are two typical Allan Variance plots. These cover a total uninterrupted time period of approximately 72 days. All other Allan Variance test runs were of shorter duration. The dashed line with a fixed slope starting at the bottom of the graph represents the computer estimated drift between the maser pair.[2] The measured output drift (see previous section) for the 3 masers involved during the same time period are:

DSN-2 $- 1.2 \times 10^{-14}$/Day @ Line Q = 6.7×10^{8}, P.O. = -88.2 DBM

NR-4 $- 8.6 \times 10^{-15}$/Day @ Line Q = 1.7×10^{9} P.O. = -101.0 DBM

SAO-14 $+ 6.5 \times 10^{-15}$/Day @ Line Q = 1.65×10^{9}, P.O. = -97.5 DBM

These masers reach a minimum noise level at about a 2000 second sampling period (τ). Systematic effects dominate at a τ of about 300,000 seconds. It appears that if a maser is used as a clock only, continuous flux gate tuning could be appropriate. The data shown in Figures 17 and 18 is for the pair sigma. Figures 19, 20, 21 show the Allan Variance for each maser of the set SAO-14, NR-4 and DSN-2. This data was obtained from pair data that resulted in comparing all of the above hydrogen masers with each other. "Three Corner Hat" analysis basically involves solving the three simultaneous equations given by the pair data for each maser. All the pair data must be measured at the same time to give satisfactory results and the number of samples should be large at each value of tau. The spreading of the calculated values at the higher taus is to be expected since the number of samples is lower and a well convergent value has not been reached.

6. Power Spectral Density of Phase

The masers were measured in pairs and the data for each individual maser was derived from the pair data. One maser in each pair was adjusted so that its output signal was in quadrature with respect to the other. These signals were mixed and analyzed with a fast fourier transform spectrum analyzer. Measurements were taken at the 5 and 100 MHz outputs. The noise as a function of offset from the carrier is plotted in Figures 22 and 23. Comparison of four masers with each other yields six sets of data, each maser appears as one of the pair in three of those sets. The best noise characteristic curve was selected from the three and arbitratily assigned to the maser. This method is justified in that the standard technique of solving simultaneous equations yields calculation errors which grow enormously with the measurement errors and with the disparity in absolute noise level of the various sources. Although this method has its own intrinsic problems, it is considered to be reasonably conservative for this application.

9. Correlation of Measured Parameters

In order to gain additional insight into the dependence of maser performance on environmental parameters, the auto and cross correlation matrices were computed for all possible combinations of data sets. This data was collected during the uninterrupted 72 day Allan Variance test. The most significant finding was a strong correlation between output frequency and dew point for two of the four masers (NR-4 and DSN-2) as shown in Figure 26.

Table 2 shows the four test masers dew point coefficient and the delay after change of dew point. From this table it can be determined that only DSN-2 and NR-4 had a significant response to dew point.

The cause of this correlation between humidity and output frequency has not been resolved at this time.

10. Reliability and Repairability

All problems and malfunctions were carefully logged during the test period. Most discrepancies were found during the initial verification tests. It seemed appropriate to categorize and separate the problems into two groups in order to gain some realistic insight into the reliability of these masers.

Table 3 summarizes the findings regarding maser reliability. It is expected that with the knowledge gained by this evaluation substantial testing will be performed before masers are released to the field and problems such as in Group I will have been corrected at the manufacturers facility. It is obvious that vacion pump failures constituted the most serious problem affecting time out of service. Other than that, the masers promise to be quite reliable.

CONCLUSIONS

The extensive series of tests which were run as part of this program yield the most definitive set of data to date on performance and operability of the Hydrogen maser frequency standard. Based on the data, the experimenters conclude that the tested masers indicate that the state of the technology provides frequency stability of about 1×10^{-15} over 1000 to 2000 seconds under conditions of an extremely well controlled environment. As a frequency standard, the Hydrogen masers are a factor of 100 better than the best Cesium standards available for short term stability. In terms of long term stability, the tests indicate that the masers age at the rate on the order of 10^{-14} per day and are retunable to better than 10^{-13}.

During a 48 day test period the masers were manually tuned four times while the frequency was continually monitored. Figure 24 is a plot of the frequency difference between NR-4 and SAO-14. The data was derived from daily phase measurements and no corrections or offset changes were made. After the masers were initially tuned they drifted apart at a rate which was determined earlier. (Refer to paragraph 4e) (Output frequency vs. Time). The masers were tuned 3 more times during the 48 day period as indicated by arrows at the top of the chart. The data shows that the measured tuning repeatability is better than predicted for this pair. One can see the clean time residuals and the characteristic parabolas for the pair of masers in Figure 25.

8. Absolute Calibration Against NBS

In order to continually track long term stability, we calibrated each maser with reference to NBS. Each hydrogen maser's output frequency can be arbitrarily set by means of the receiver synthesizer, cavity frequency and cavity magnetic field bias. For calibration purposes each maser cavity was tuned as precisely as possible. The typical output frequency uncertainty is $\pm 3 \times 10^{-14}$ due to cavity mistuning. The magnetic field bias was specified and the corresponding Zeeman frequency measured. Each maser receiver synthesizer was then set to a value that produced an output frequency equivalent to the national standard. The process involved maintaining a Cesium frequency standard ensemble as the local reference against which the masers were measured. The ensemble offset from NBS was determined by making several clock trips to NBS with a portable Cesium standard. At the test conclusion the "standard" synthesizer setting was thus determined for each maser. The particular synthesizer settings derived for the two test masers, given tuned cavities are:

Maser	Synthesizer Setting	Zeeman Frequency
NR-4	5751.689467 Hz	400 Hz
SAO-14	405751.68900 Hz	700 Hz

It should be noted however that when a maser physics unit is opened up and a new storage bulb or teflon coating is installed the calibration becomes void. Furthermore, there is evidence the maser output frequency changes without a corresponding change in cavity frequency or Zeeman frequency. Additionally we have found that when a maser is opened up for vacion element replacement the maser's output frequency may or may not be affected due to some unknown mechanisms. A maser calibration, however useful over the short term, may be of limited value for long term purposes. The calibration uncertainty of this experiment is estimated to be $\pm 1 \times 10^{-13}$.

Environmental factors can affect a maser output frequency by as much as a part in 10^{14}. This suggests that to obtain the ultimate performance available, the masers must be kept in an environment 10 times more stable than that of a normal office or laboratory. Additional work is needed to characterize and explain and then to correct the, as yet, mysterious dependence of frequency upon humidity.

Finally, the Hydrogen masers appear to be limited in reliability by their vacuum systems. The vacion pumps proved to be a continuing problem. Nevertheless, when subjected to a very protected environment, the masers were surprisingly reliable, showing a "down-time" of less than 2.5%.

ACKNOWLEDGEMENTS

The authors wish to acknowledge the contribution of several individuals to this report. Roland Taylor and Donald Bodkin of JPL were involved in the testing of the masers and the operation of the entire test facility. JPL's Charles Greenhall, Roger Meyer, Earl Endsley, Philip Clements and Phuong Tu supported the effort with analysis, special tests and data processing.

REFERENCES

[1] D. W. Allan, "Statistics of Atomic Frequency Standards," Proc. IEEE, vol. 54, pp. 221-230, February 1966.

[2] C. A. Greenhall, "Removal of Drift from Frequency Stability Measurements," JPL-TDA Progress Report, 42-65, pp. 127-132, 1981.

Table 1. Tests Performed

1. VERIFICATION OF INPUTS, OUTPUTS, PROPER FUNCTIONING OF CONTROLS
2. I.F. METER CALIBRATION
3. PRESSURE CONTROL SETTING DEPENDENT PARAMETERS
   BASELINE FOR RELATIONSHIP OF LINE-Q, POWER OUTPUT, PRESSURE
4. ENVIRONMENTAL TESTS:
   a. OUTPUT FREQUENCY VS. AC/DC INPUT VOLTAGE
   b. OUTPUT FREQUENCY VS. AMBIENT MAGNETIC FIELD
   c. OUTPUT FREQUENCY VS. AMBIENT TEMPERATURE
   d. OUTPUT FREQUENCY VS. AMBIENT BAROMETRIC PRESSURE
   e. OUTPUT FREQUENCY VS. TIME
5. FREQUENCY STABILITY - ALLAN VARIANCE $1s < \tau < 1 \times 10^6 s$
6. POWER SPECTRAL DENSITY OF PHASE
7. TUNING REPEATABILITY
8. ABSOLUTE CALIBRATION AGAINST NBS
9. CORRELATION OF MEASURED PARAMETERS
10. RELIABILITY AND REPAIRABILITY ASSESSMENT

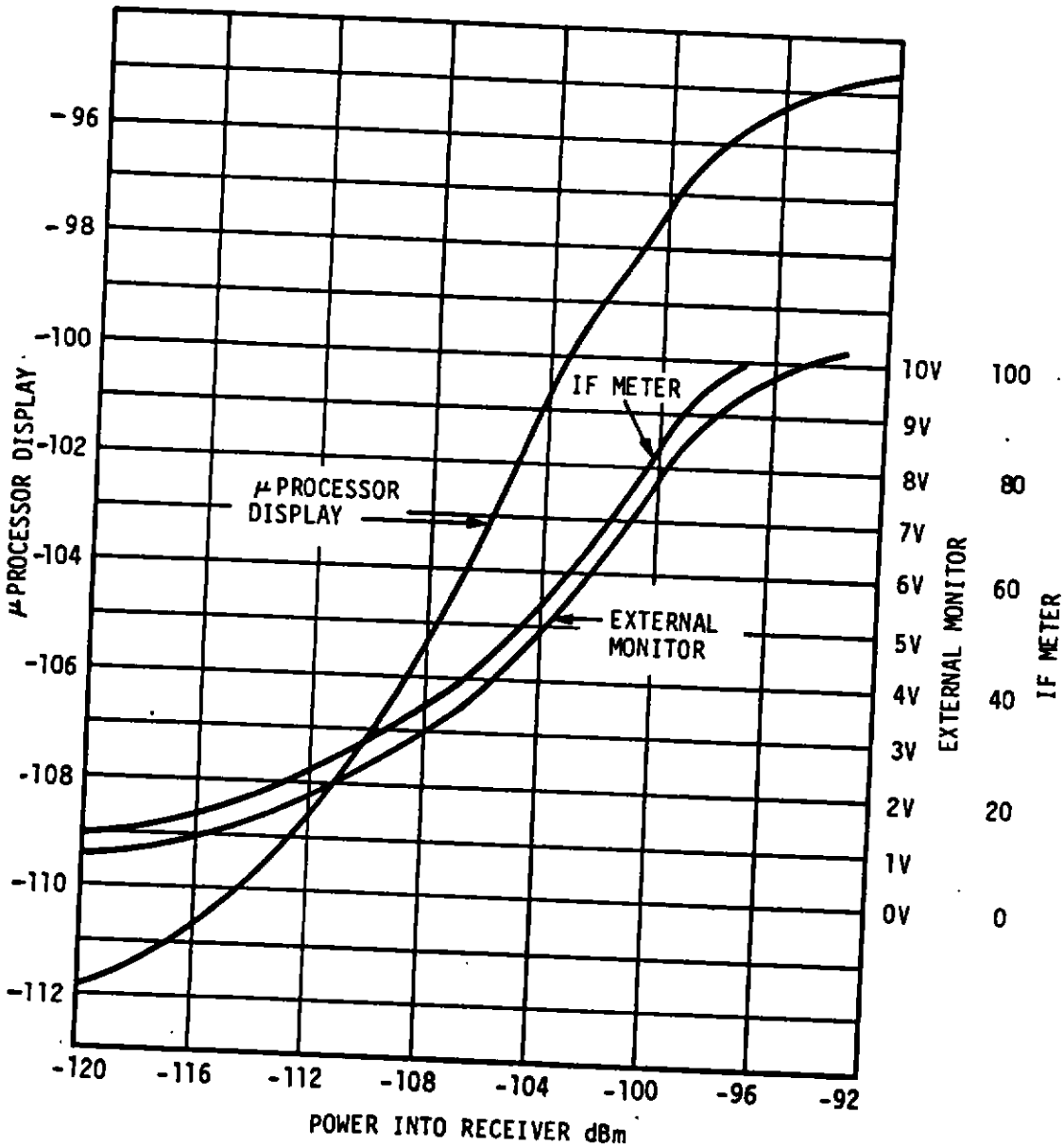

Figure 1. NR-4 Output Power Calibration

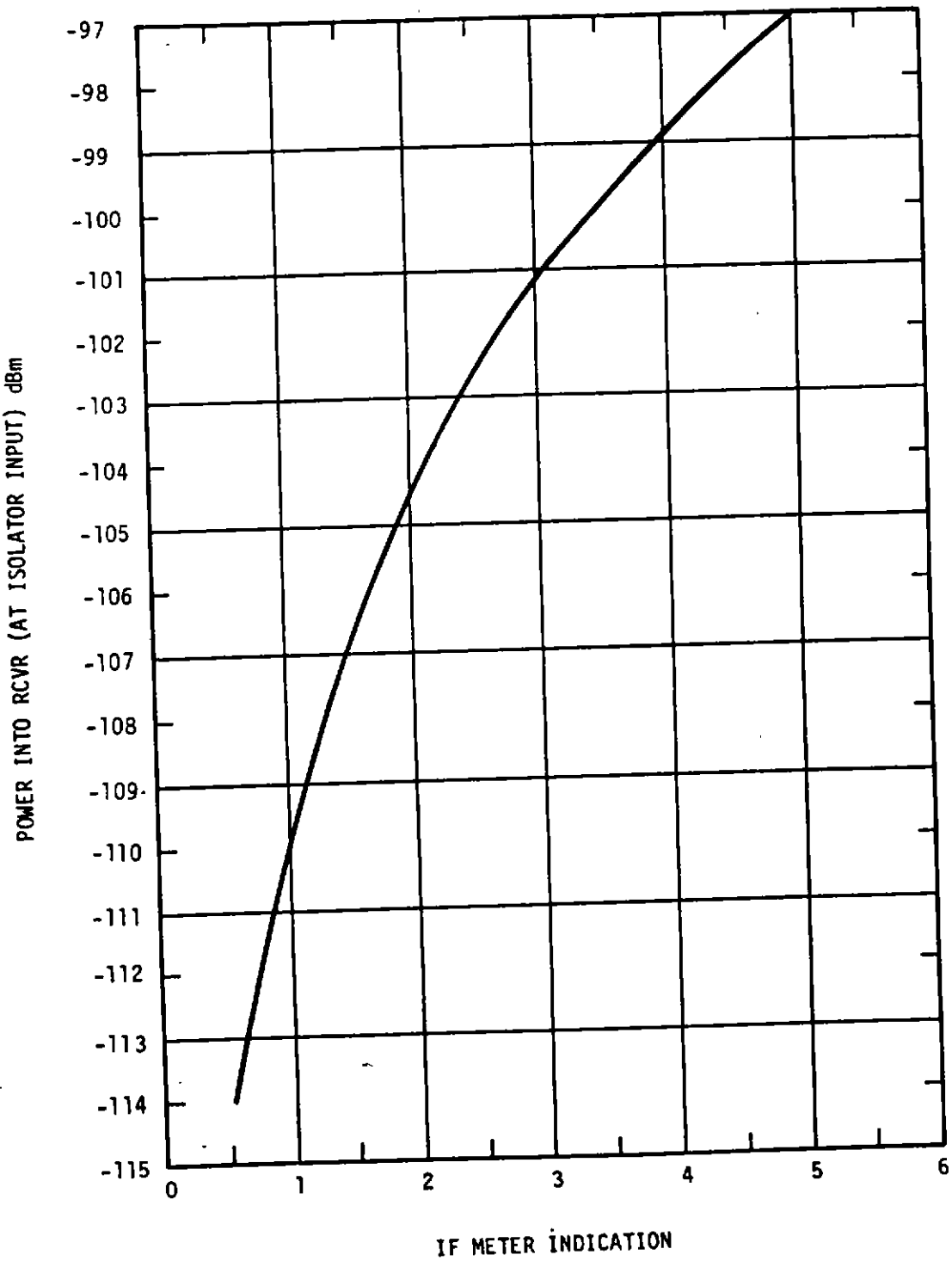

Figure 2. SAO-14 Output Power Calibration

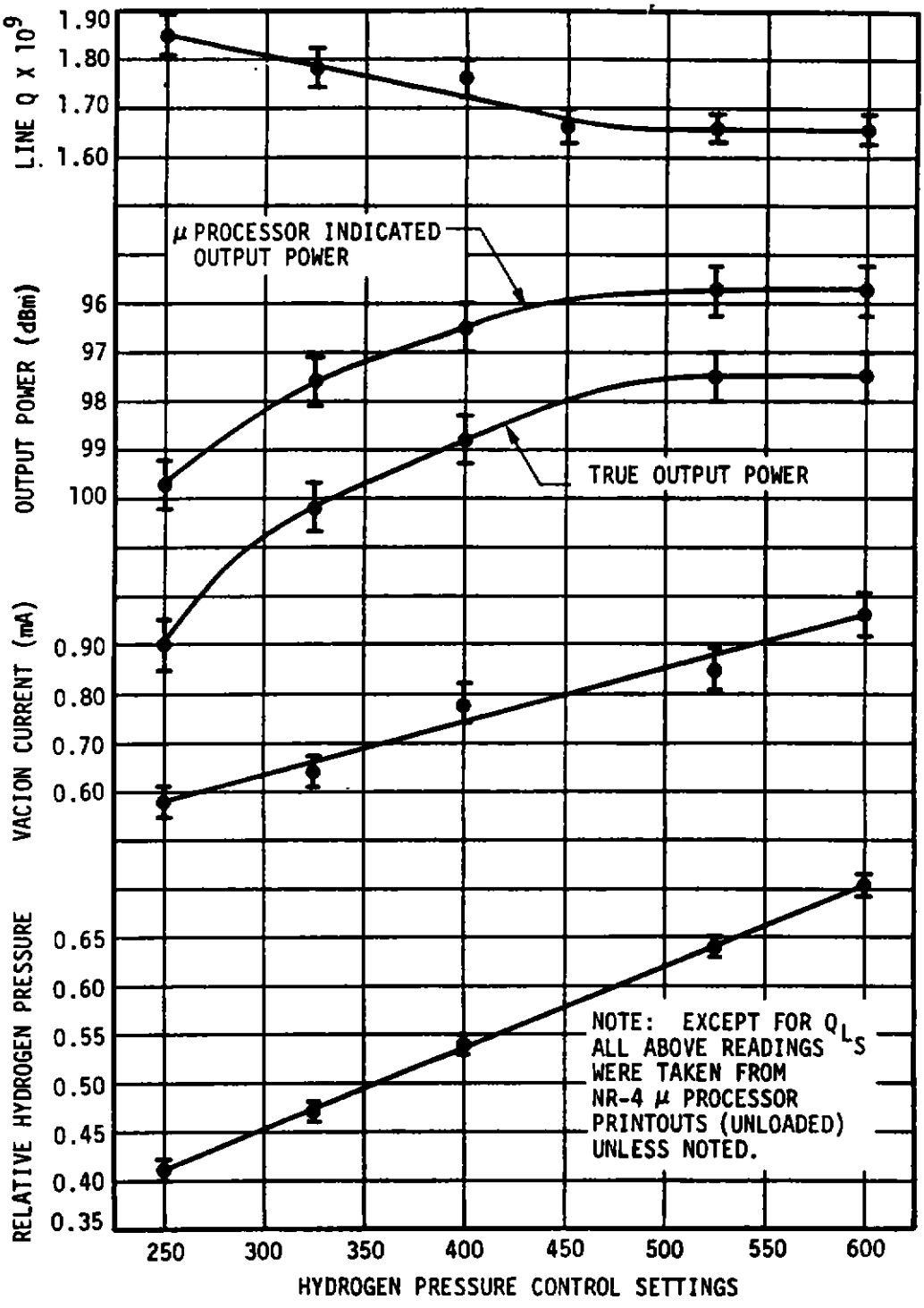

Figure 3. NR-4 Pressure Dependent Parameters

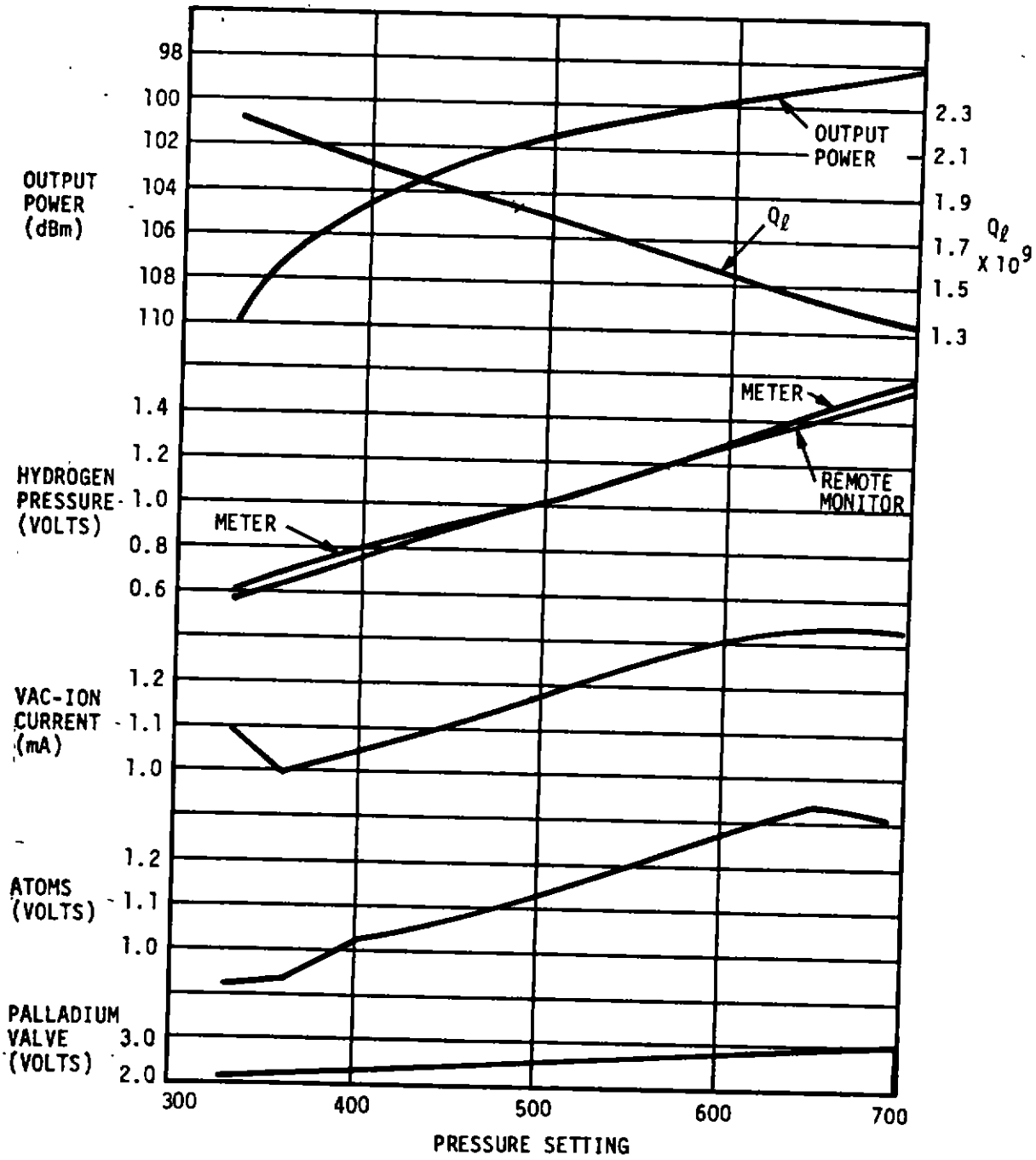

Figure 4. SAO-14 Pressure Dependent Parameters

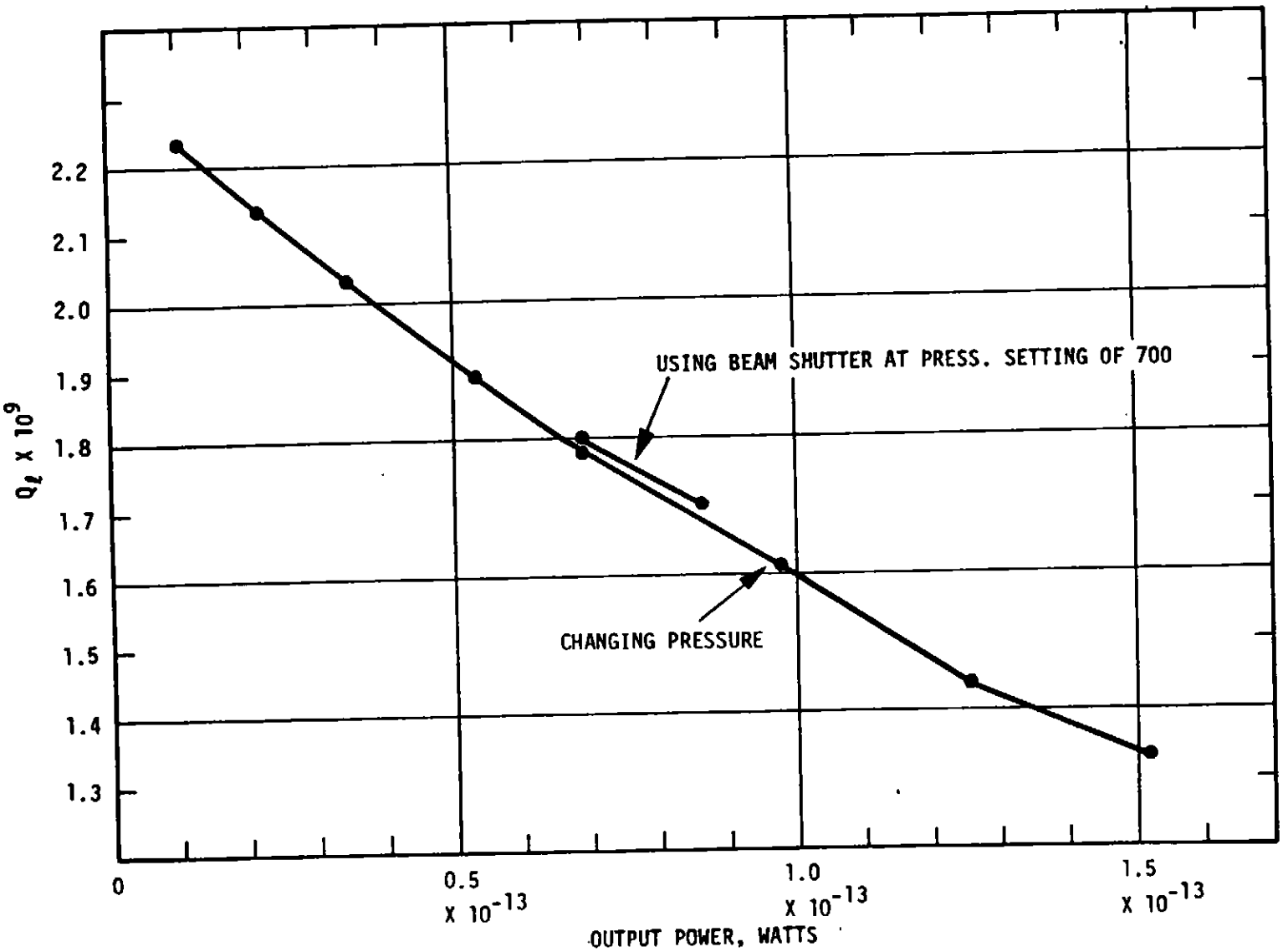

Figure 5. SAO-14 Line Q vs Output Power

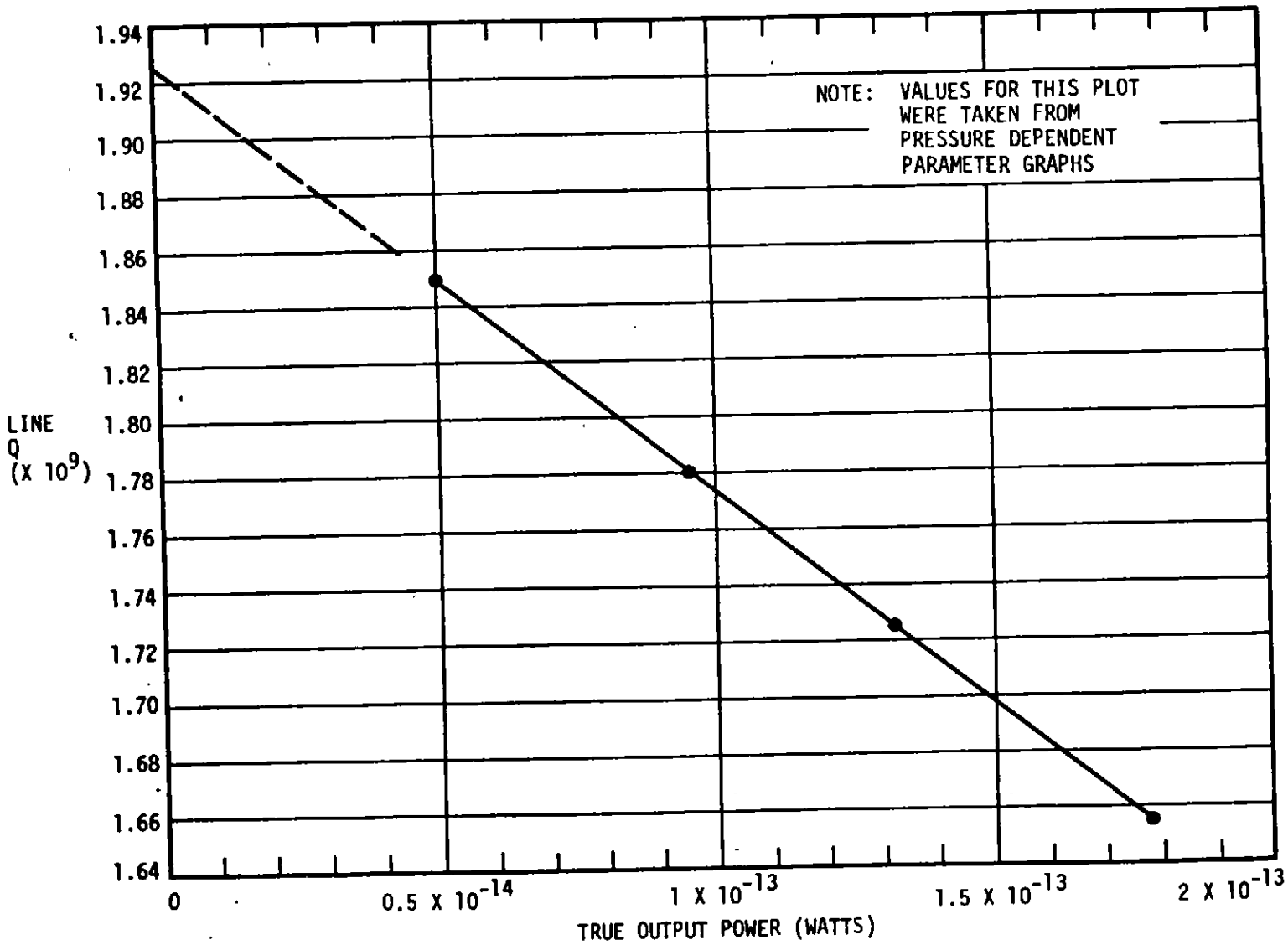

Figure 6. NR-4 Line Q vs Output Power

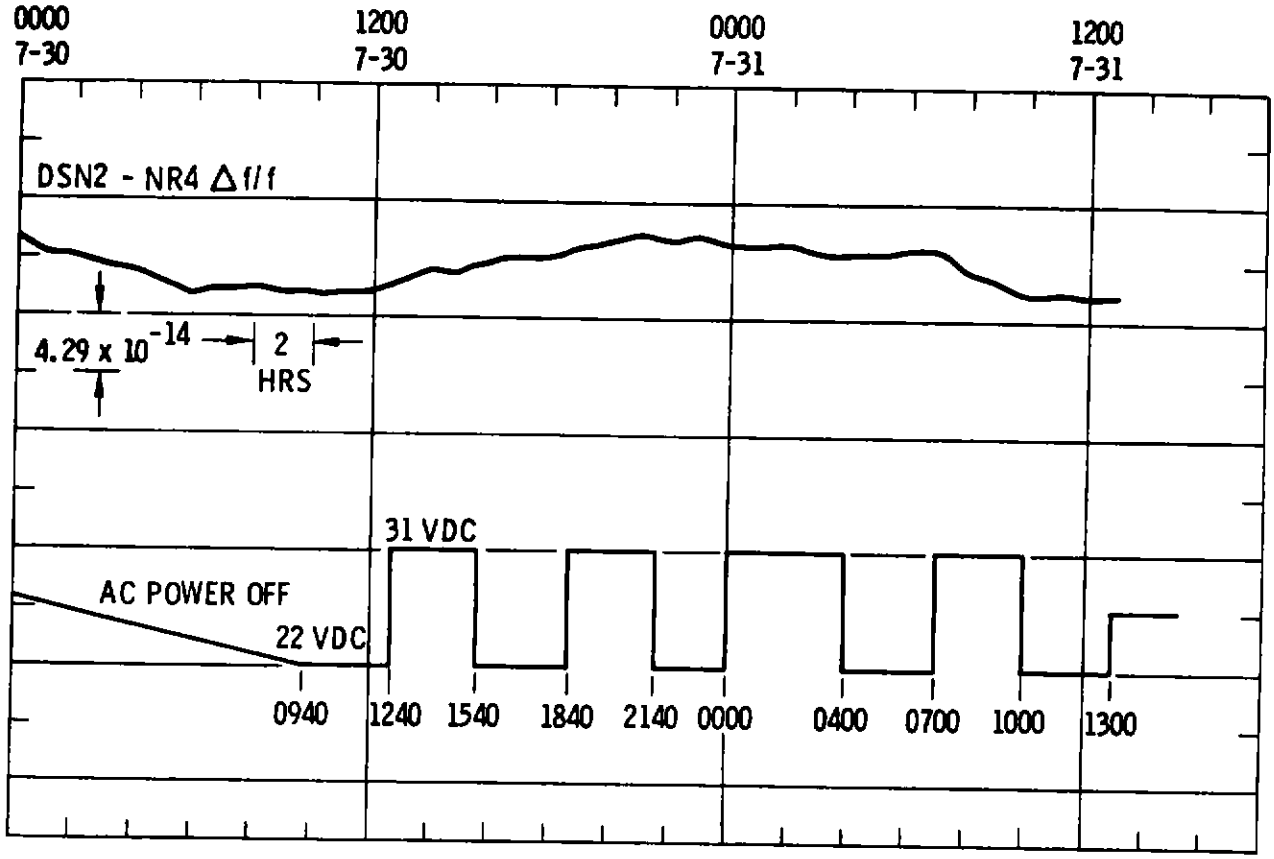

Figure 7. NR-4 Output Frequency Shift vs DC Input Voltage

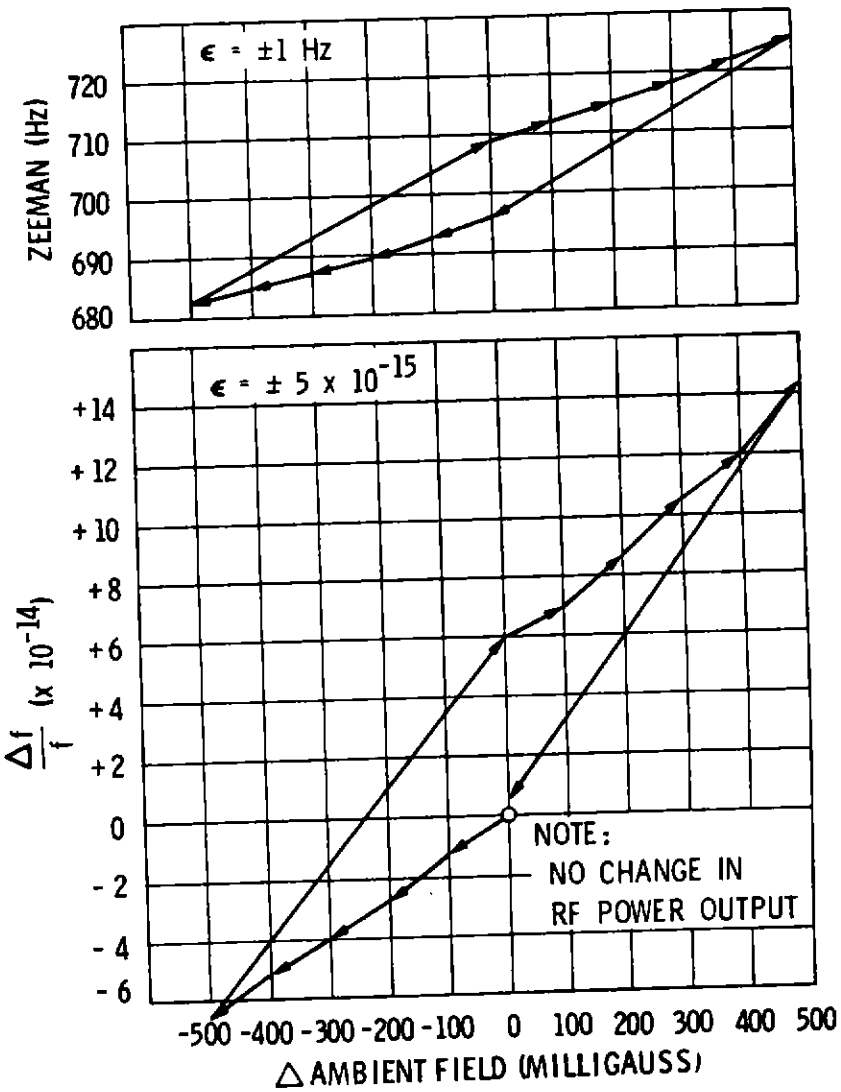

Figure 8. SAO-14 Magnetic Field Test - 1st Series

MAGNETIC FIELD	FRACTIONAL FREQ SHIFT PER GAUSS		
	HYDROGEN PRESSURE CONTROL SET TO 325, LOW FLUX	HYDROGEN PRESSURE CONTROL SET TO 525, NORMAL FLUX	HYDROGEN PRESSURE CONTROL SET TO 600, HIGH FLUX
200 mG PEAK TO PEAK	5.88×10^{-14}	8.01×10^{-14}	7.71×10^{-14}
600 mG PEAK TO PEAK	5.71×10^{-14}	5.53×10^{-14}	5.96×10^{-14}
1000 mG PEAK TO PEAK	4.49×10^{-14}	5.06×10^{-14}	4.77×10^{-14}

NOTES: 1. ALL $\Delta f/f$ VALUES HAVE AN UNCERTAINTY FACTOR OF $\pm 5 \times 10^{-15}$
2. AMBIENT TEMPERATURE = 23°C
3. ZEEMAN FREQUENCY = 400 Hz
4. THE UNCERTAINTY OF ΔH IS ESTIMATED TO BE ±5%
5. ALL MEASUREMENTS AVERAGE OF 5 STEPS

Figure 9. NR-4 Frequency Shift vs. Magnetic Field

MAGNETIC FIELD	FRACTIONAL FREQ SHIFT PER GAUSS	
	HYDROGEN PRESSURE CONTROL SET TO 360, LOW FLUX	HYDROGEN PRESSURE CONTROL SET TO 500, NORMAL FLUX
200 mG PEAK TO PEAK	1.87×10^{-13}	2.75×10^{-13}
600 mG PEAK TO PEAK	1.40×10^{-13}	2.17×10^{-13}
1000 mG PEAK TO PEAK	1.23×10^{-13}	1.88×10^{-13}

NOTES: 1. ALL $\Delta f/f$ VALUES HAVE AN UNCERTAINTY FACTOR OF $\pm 5 \times 10^{-15}$
2. AMBIENT TEMPERATURE = 24°C
3. ZEEMAN FREQUENCY = 700 Hz
4. THE UNCERTAINTY OF ΔH IS ESTIMATED TO BE ±5%
5. ALL MEASUREMENTS AVERAGE OF 5 STEPS

Figure 10. SAO-14 Frequency Shift vs. Magnetic Field

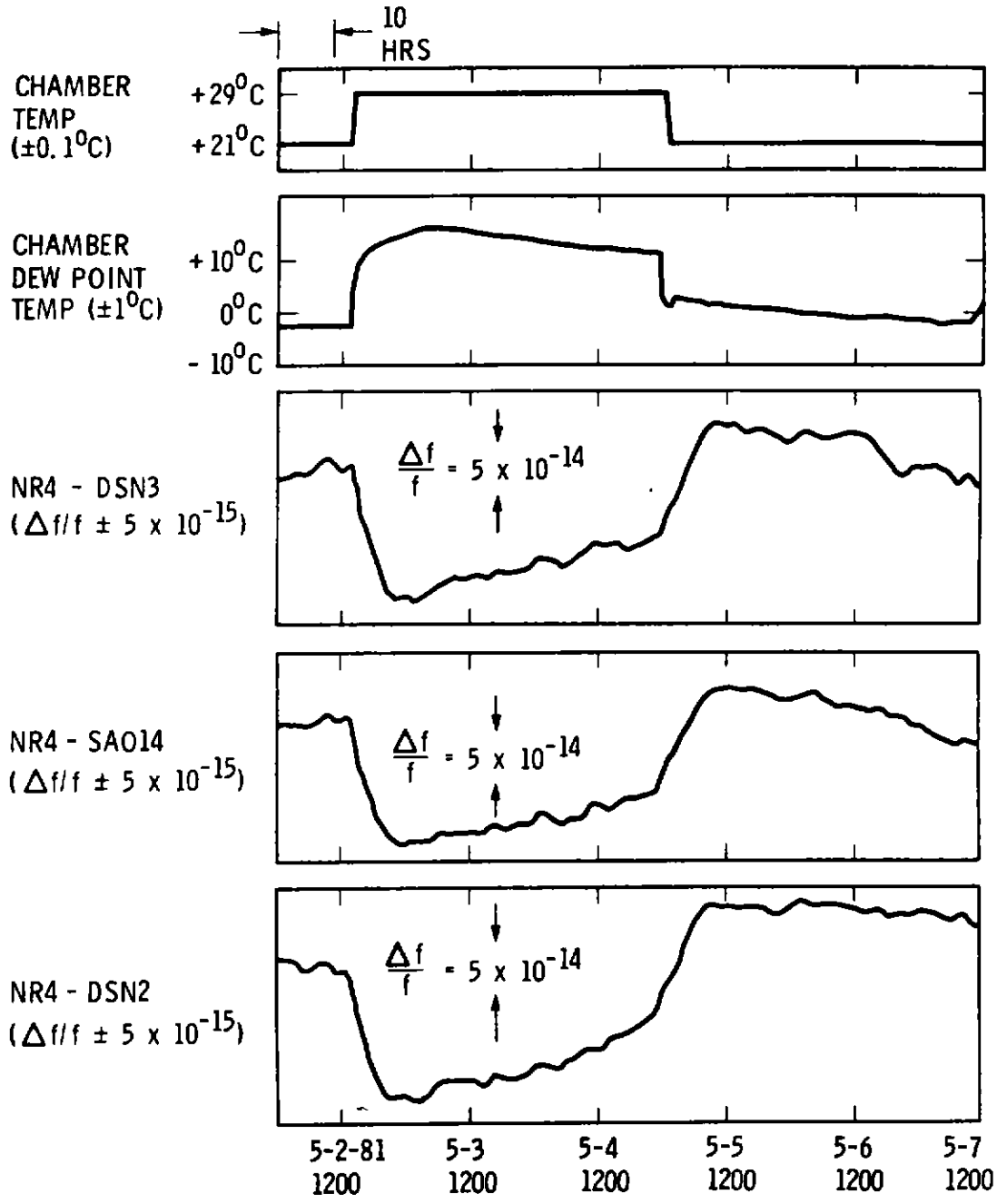

Figure 11. NR-4 Temperature Test

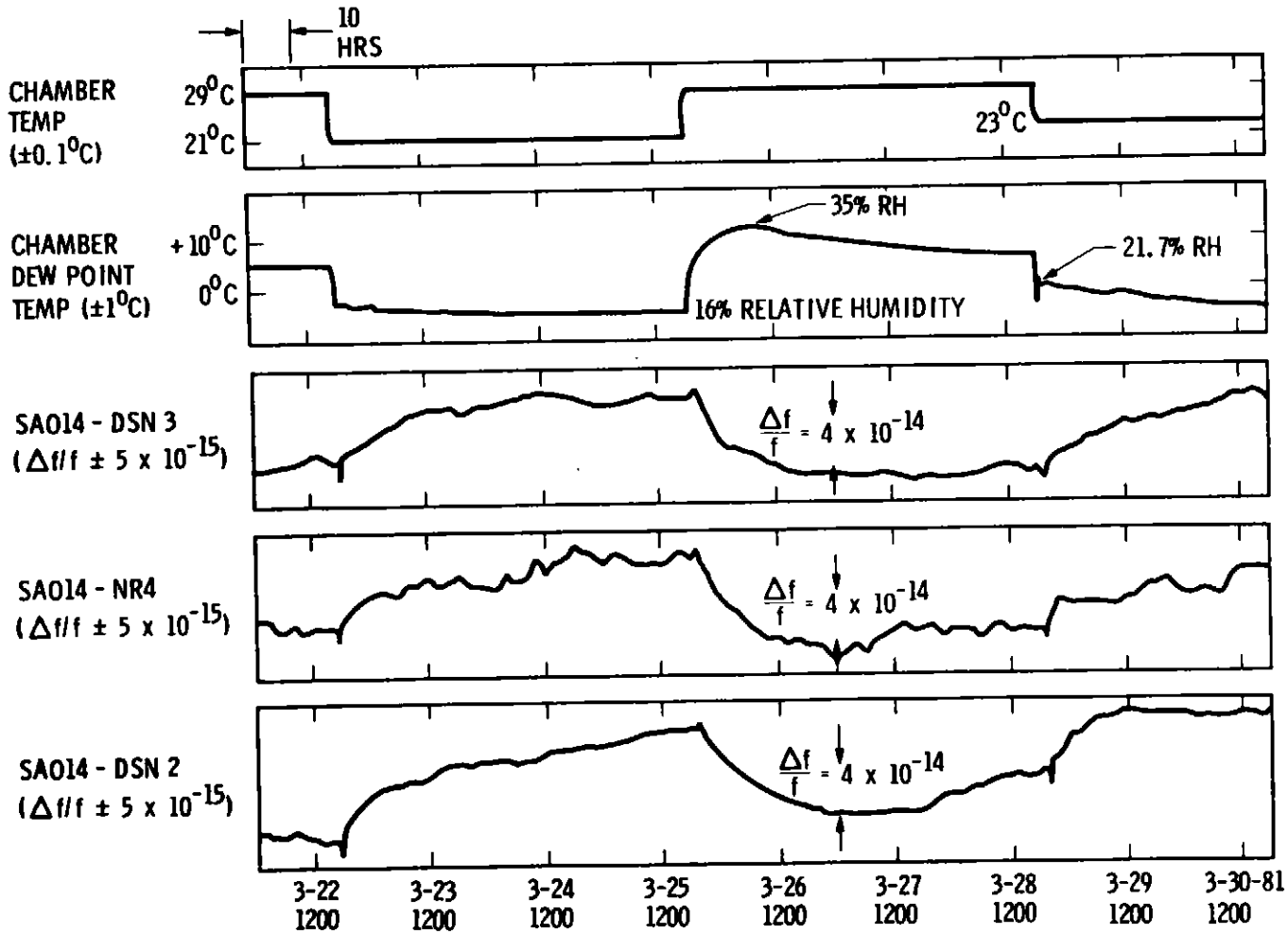

Figure 12. SAO-14 Temperature Test

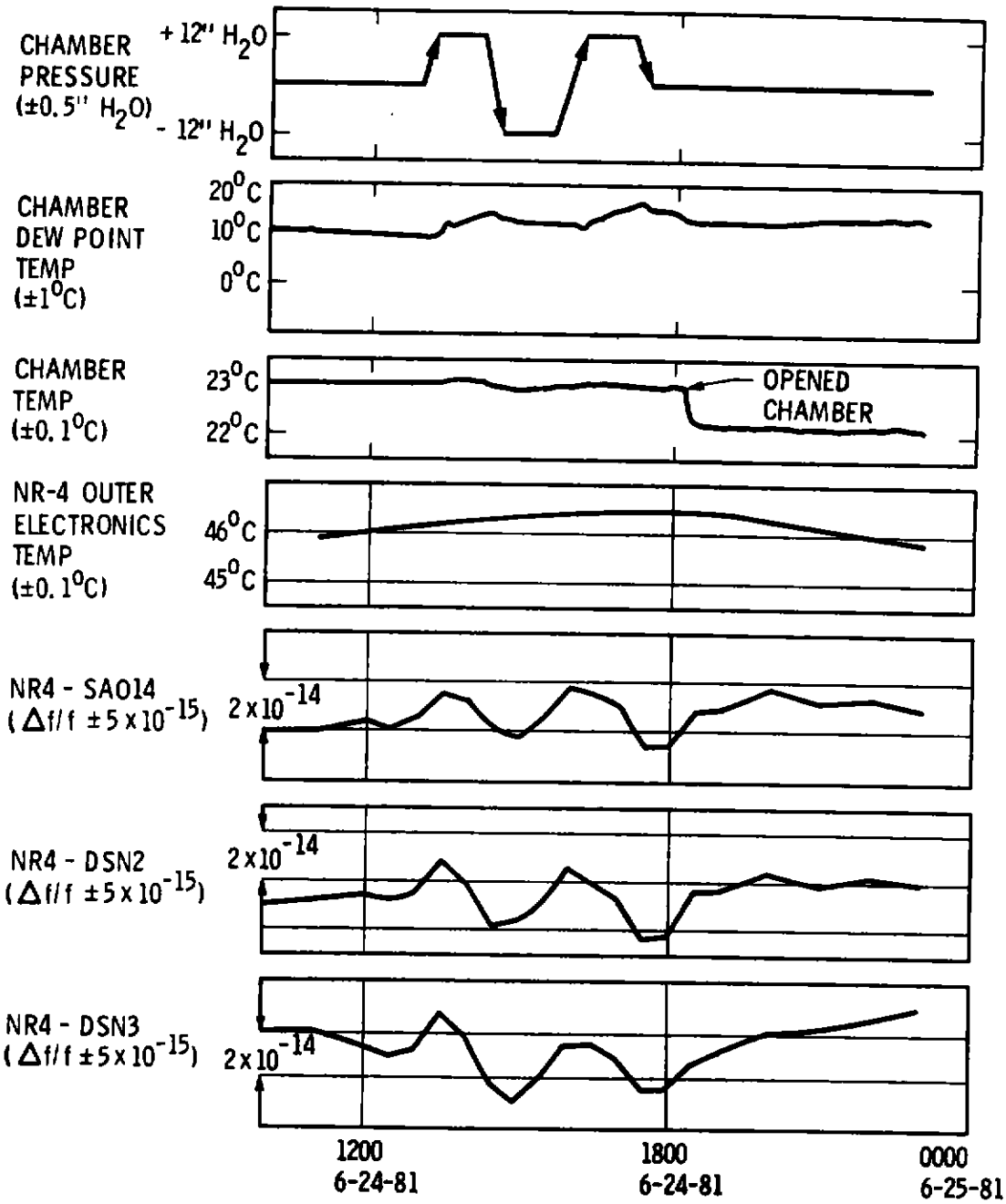

Figure 13. NR-4 Barometric Pressure Test

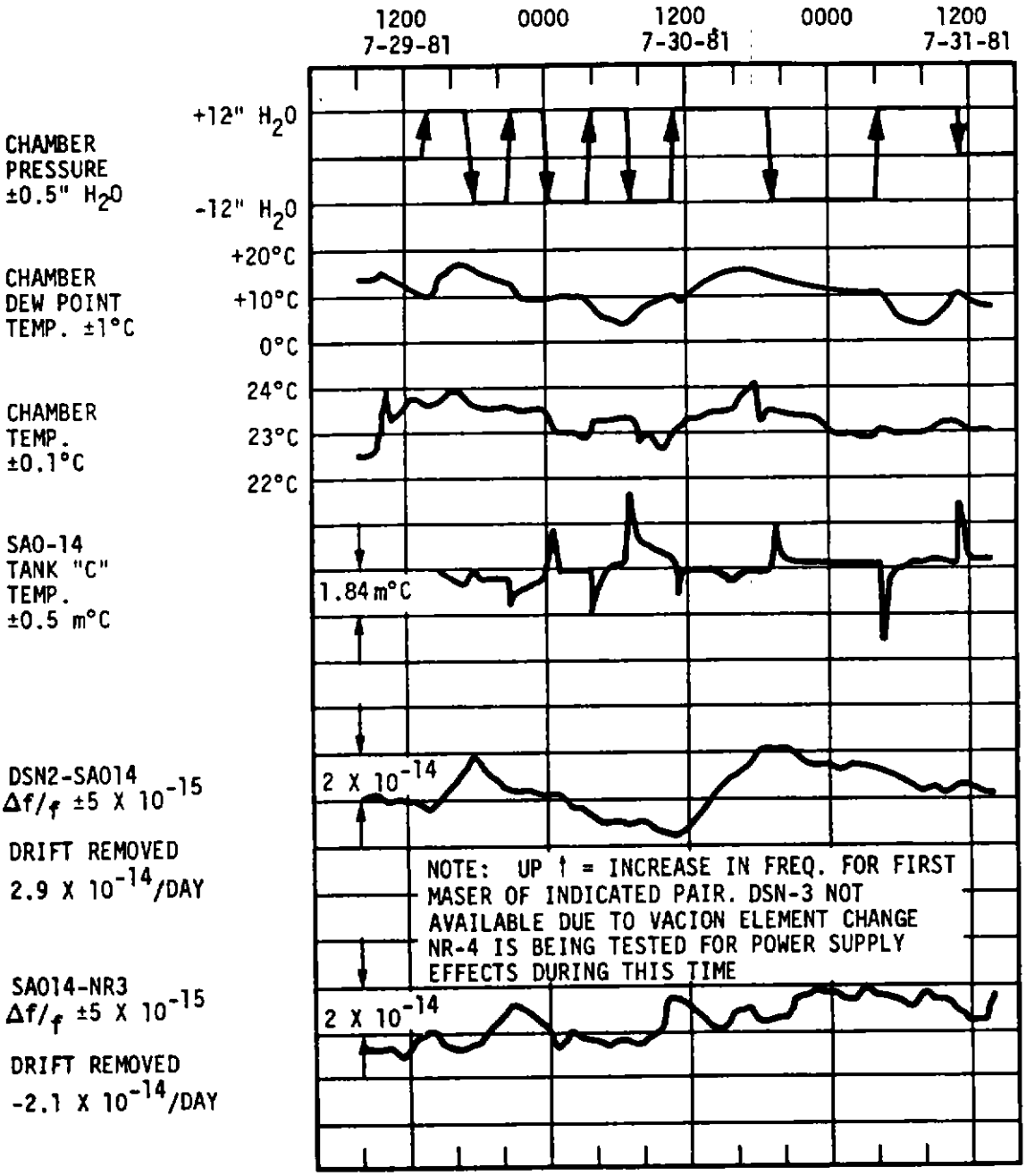

Figure 14. SAO-14 Barometric Pressure Test

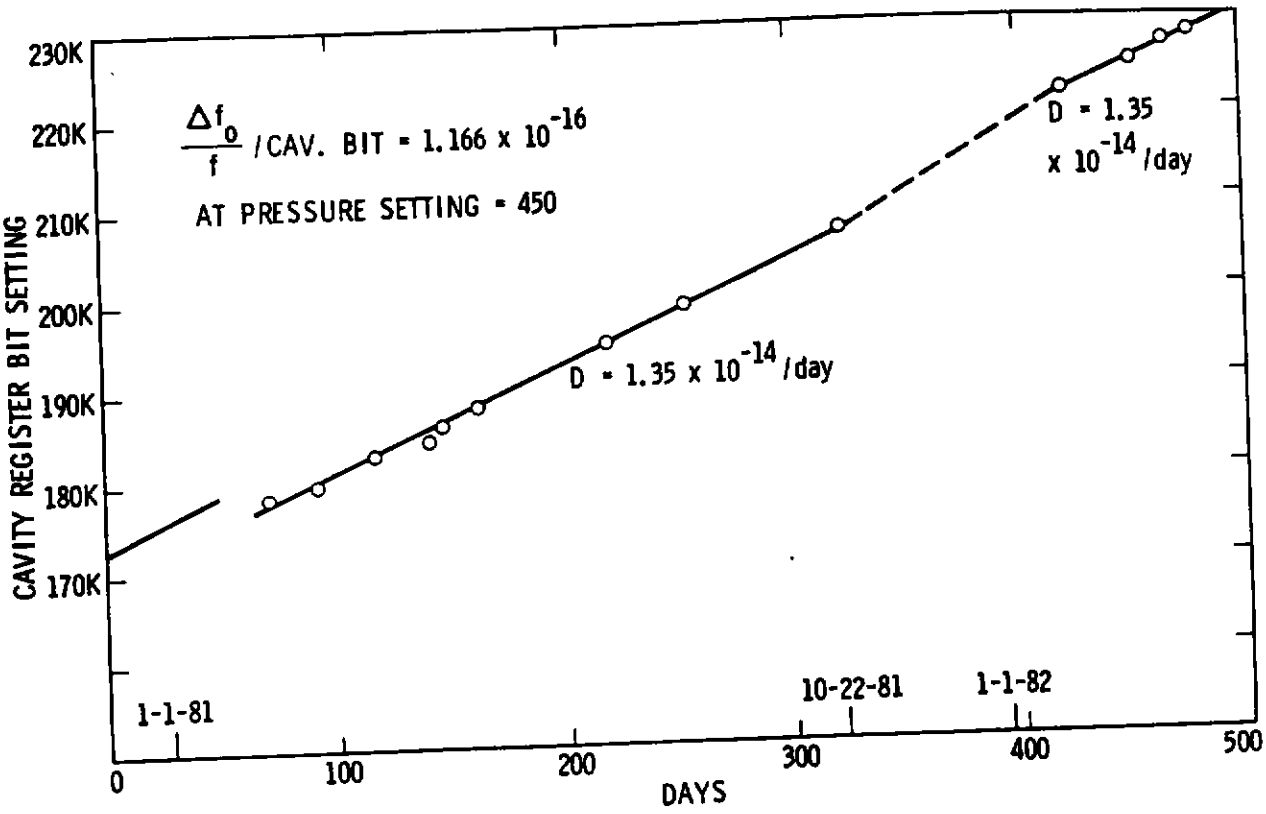

Figure 15. NR-4 Cavity Tuning

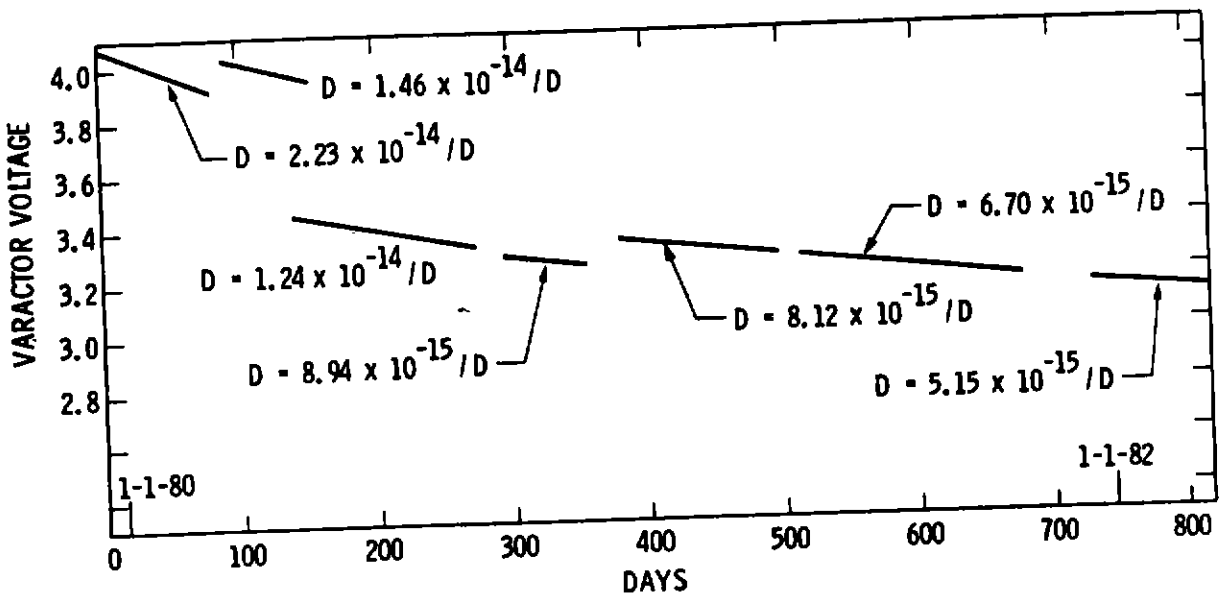

Figure 16. SAO-14 Cavity Tuning

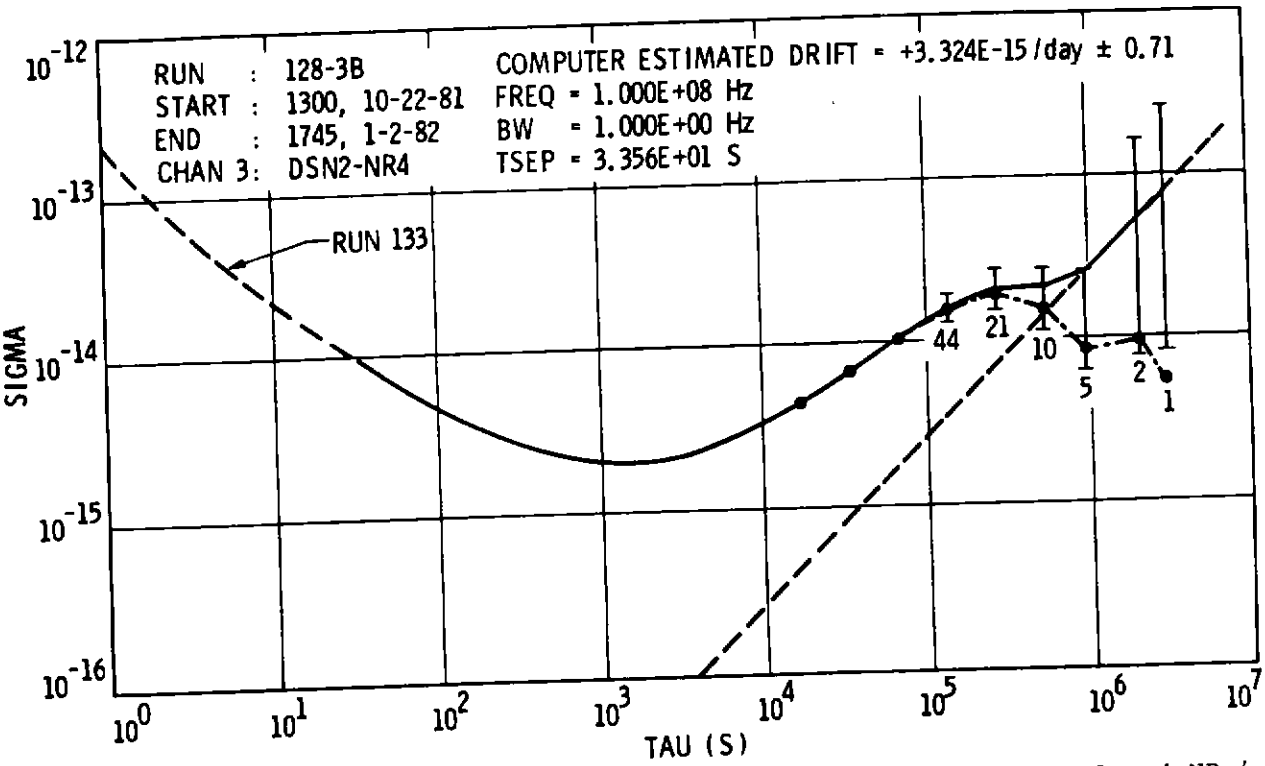

Figure 17. Allan Variance with Computed Drift Removed Between DSN-2 and NR-4

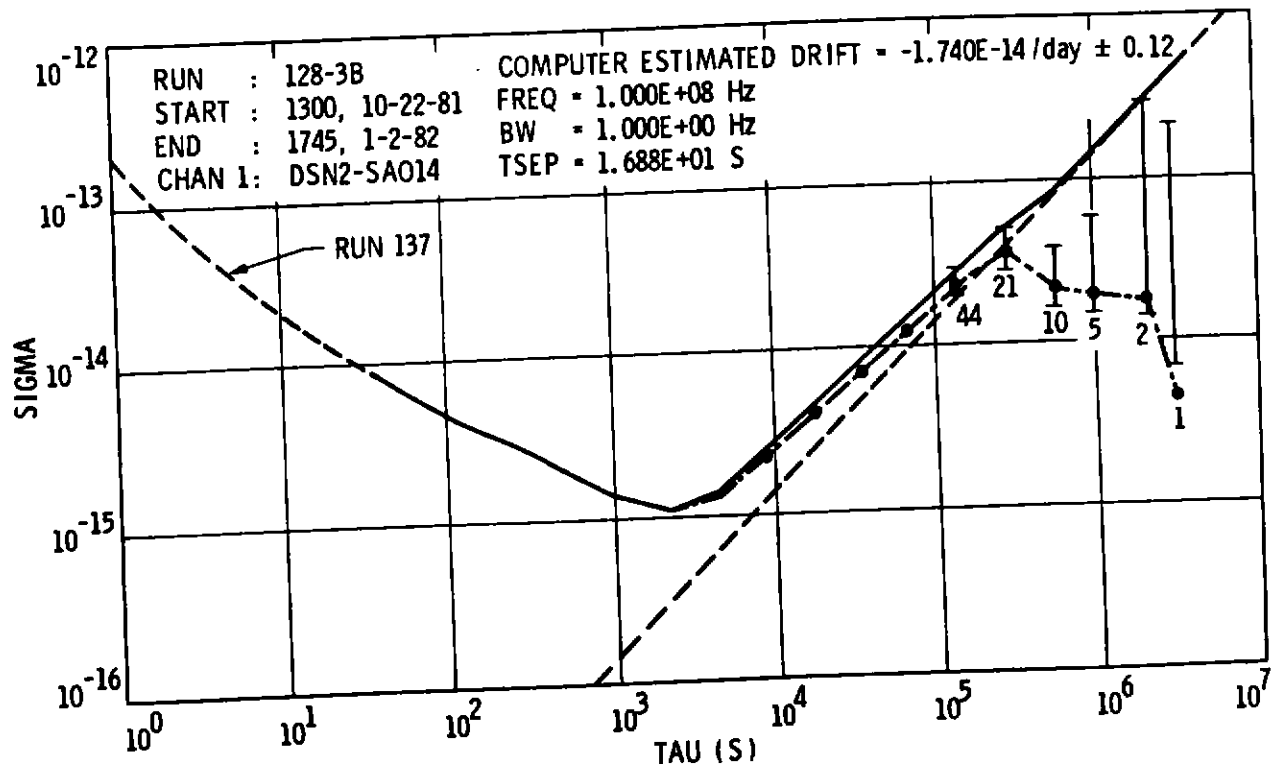

Figure 18. Allan Variance with Computed Drift Removed Between DSN-2 and SAO-14

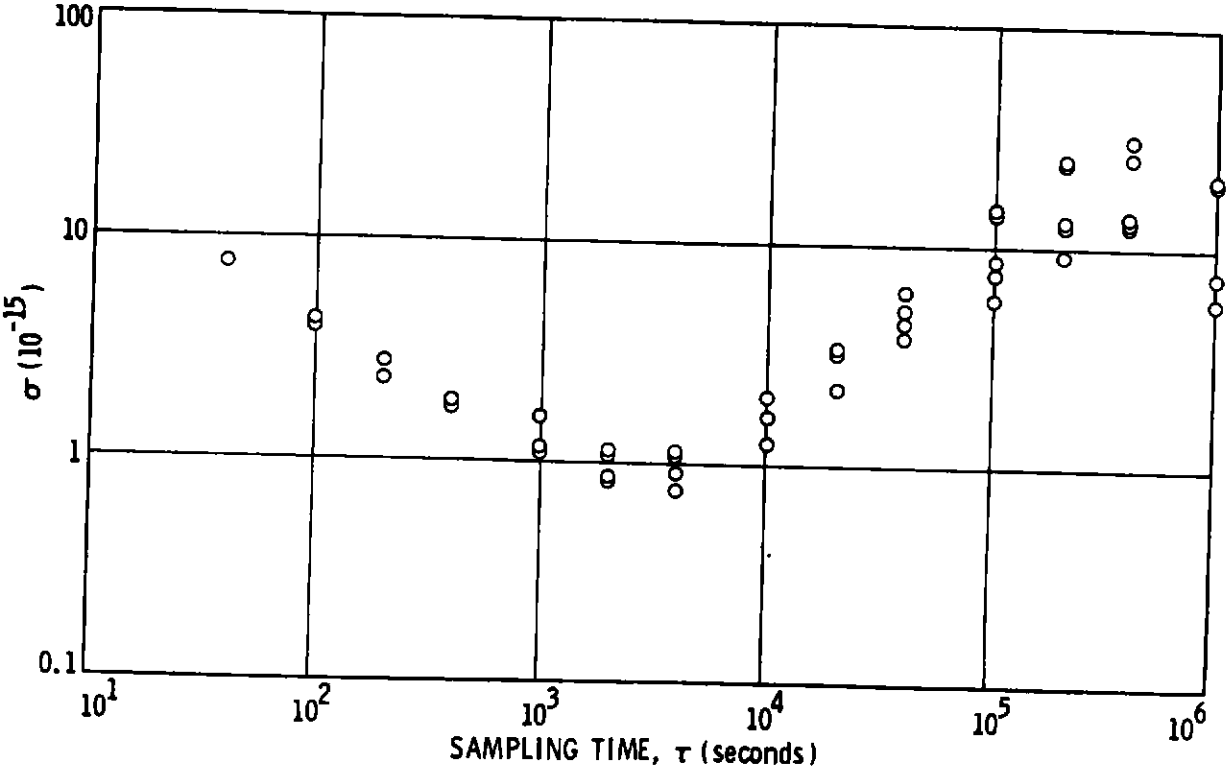

Figure 19. SAO-14 Three Corner Hat Analysis

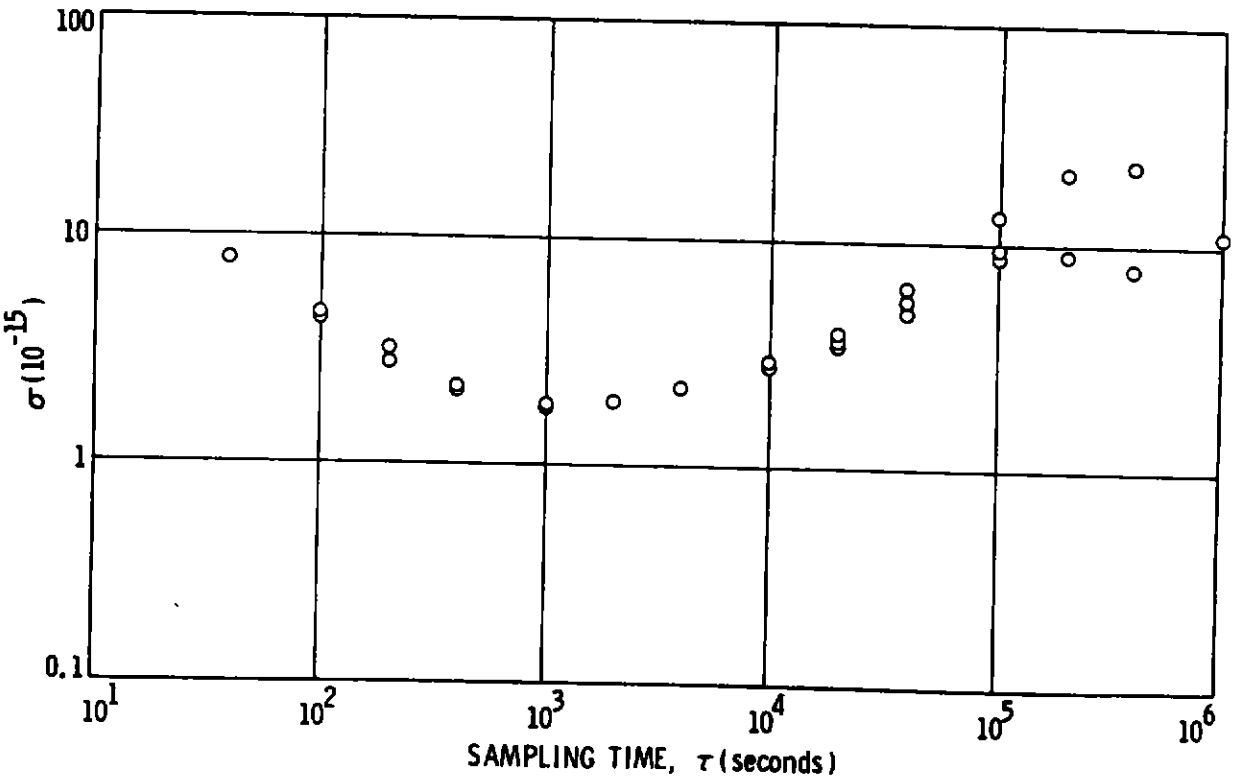

Figure 20. NR-4 Three Corner Hat Analysis

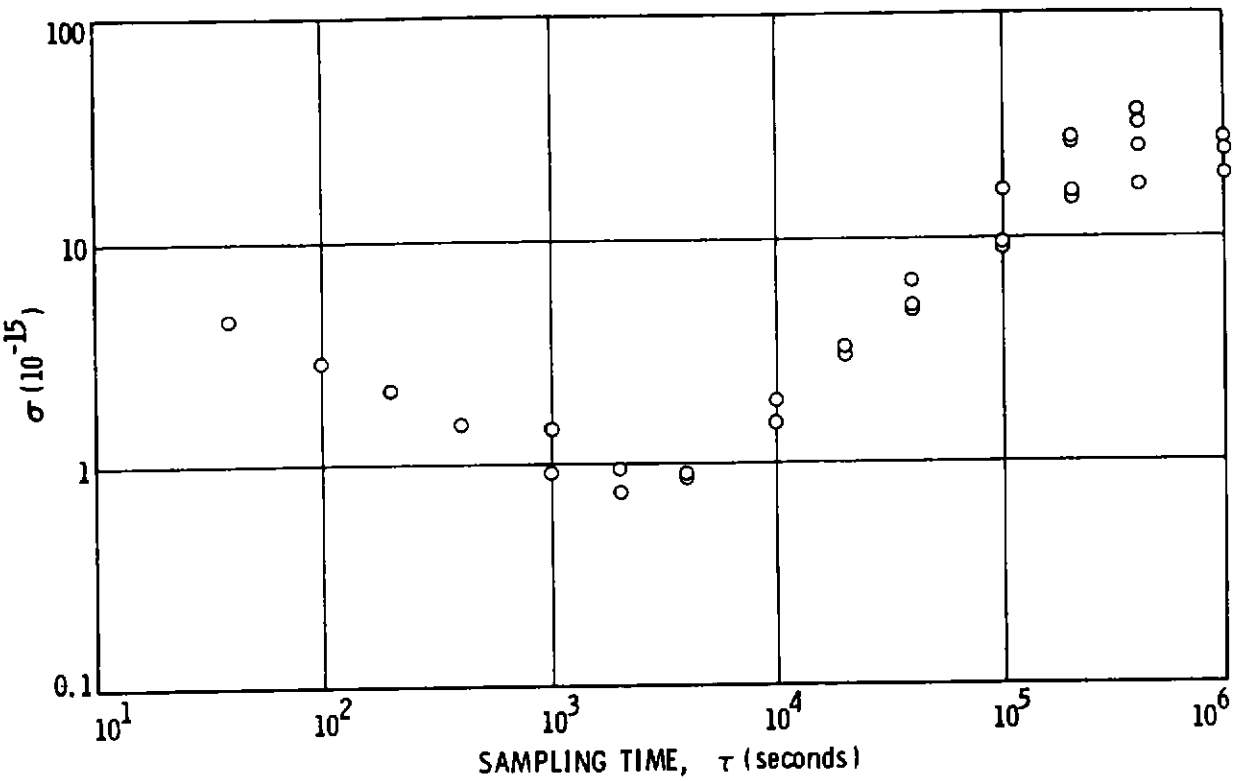

Figure 21. DSN-2 Three Corner Hat Analysis

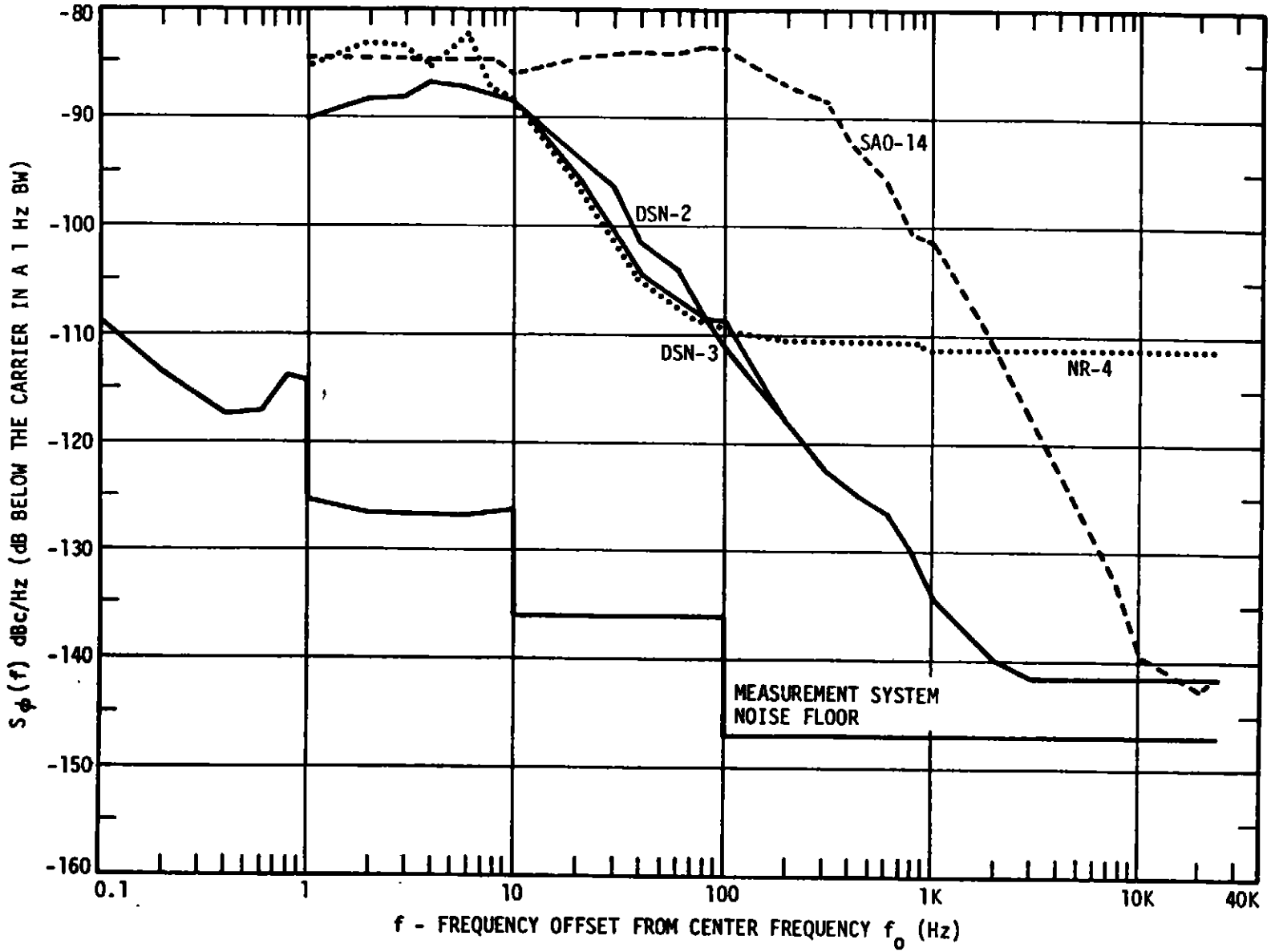

Figure 22. 100 MHz Phase Noise

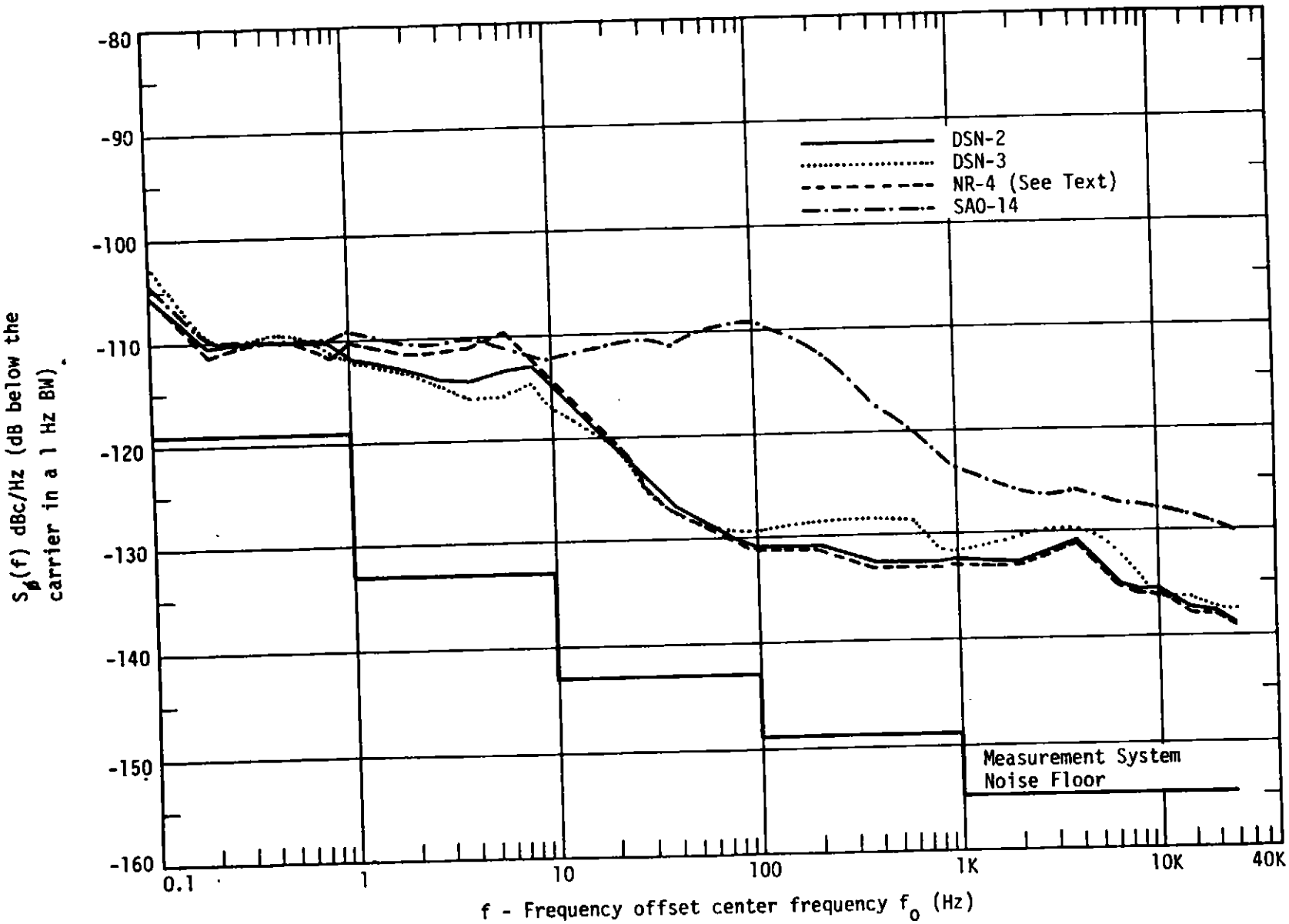

Figure 23. 5 MHz Phase Noise

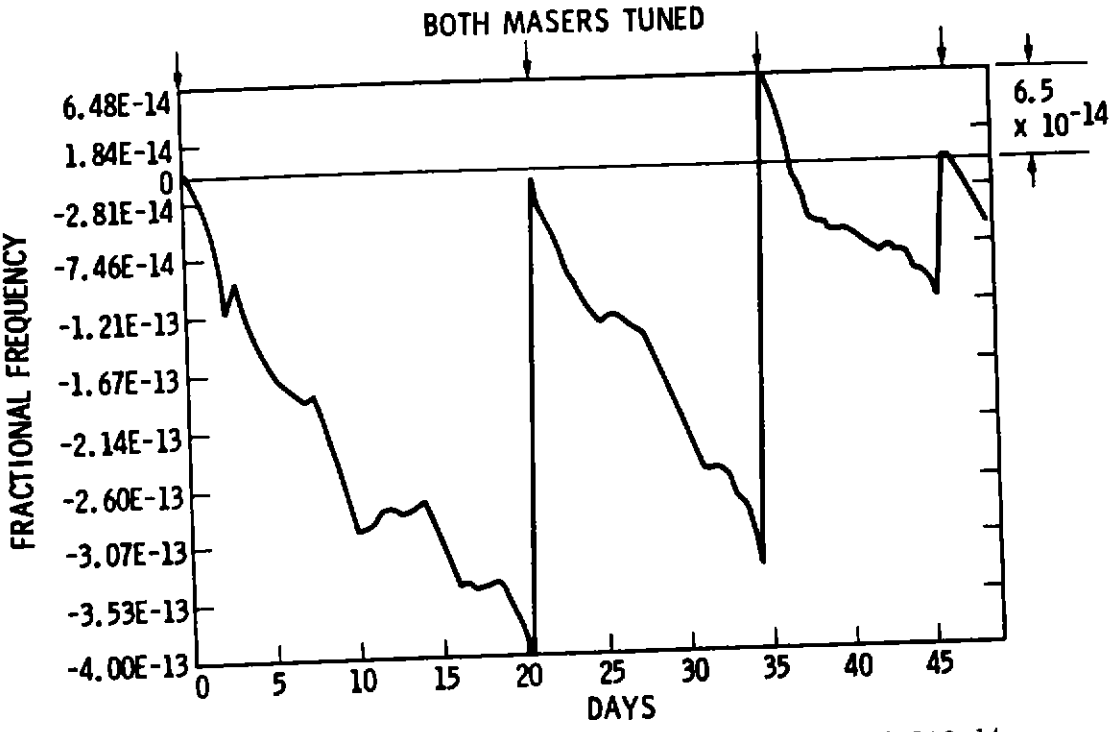

Figure 24. Tuning Repeatability of NR-4 and SAO-14

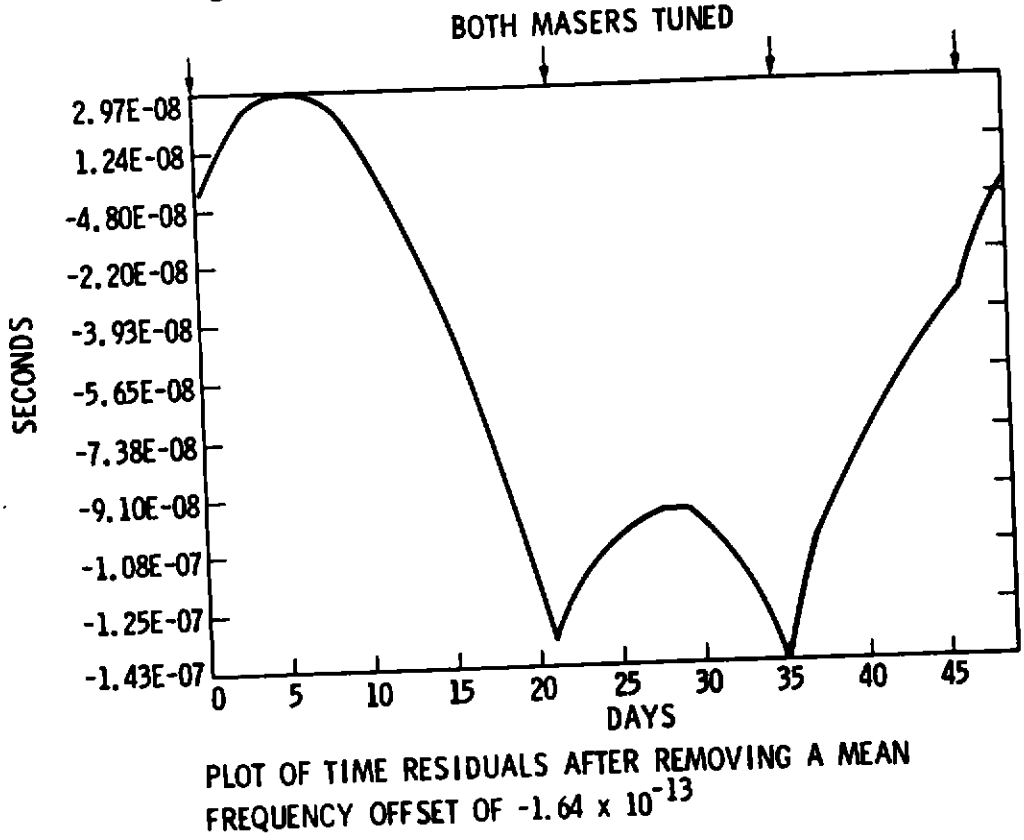

Figure 25. Time Residuals Between NR-4 and SAO-14

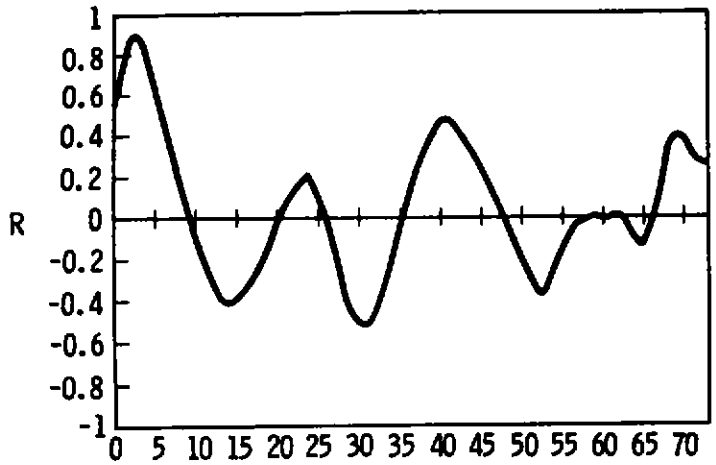

DEW POINT VS. NR-4/ DSN-3 CROSS-CORRELATION

Figure 26. Dew Point vs. NR-4/DSN-3 Cross-Correlation

Table 2. Coefficients: Masers vs. Dew Point

FREQUENCY STANDARD PAIR	R_{PEAK}	DELAY (DAYS)
NR-4/ DSN-3	0.895	1.5
SAO-14/ DSN-3	-0.729	0
NR-4/ SAO-14	0.911	1.0
DSN-2/ DSN-3	0.878	2.5
DSN-2/ SAO-14	0.861	2.0
DSN-2/ NR-4	0.789	3.5

COEFFICIENTS: MASERS VS. DEW POINT

Table 3. Reliability

			SAO-14	NR-4
GROUP I NOT AFFECTING RELIABILITY	1	PROBLEM ASSOCIATED WITH ORIGINAL CONSTRUCTION AND INSPECTION.	5; 31%	2; 10%
	2	PROBLEMS DUE TO DESIGN ERRORS OR INHERENT WITH NEW DESIGN (SOME OF THESE PROBLEMS WERE FIXED AT JPL BY MODIFICATIONS, OTHERS WERE MINOR IN NATURE AND LEFT AS IS.)	5; 31%	11; 55%
	3	"INFANT MORTALITY TYPE" COMPONENT FAILURES AS JUDGED BY THE AUTHOR.	1; 6%	0; 0%
		PERCENTAGES ESTIMATED BY AUTHOR. TOTAL	11; 68%	13; 65%
GROUP II AFFECTING RELIABILITY	4	COMPONENT FAILURES RANDOM OR RECURRING; WORKMANSHIP FAILURES.	1; 6%	3; 15%
	5	VACION PUMP FAILURE	2; 13%	1; 5%
	6	ADJUSTMENTS REQUIRED AS A RESULT OF REPAIR WORK AFTER MASER HAS STABILIZED OR AFTER MASER HAS BEEN MOVED	2; 13%	3; 15%
		PERCENTAGES ESTIMATED BY AUTHOR TOTAL	5; 32%	7; 35%

		SAO-14	NR-4
OUT OF SERVICE	DAYS OPERATING AT JPL (TO 5-31-82)	906; 100%	564; 100%
	DAYS OUT OF SERVICE DUE TO VACION PUMP FAILURE	14; 1.6%	7; 1.25%
	DAYS OUT OF SERVICE DUE TO ALL OTHER FAILURES GROUP II	3; 0.3%	7; 1.25%
	TOTAL DAYS AND PERCENTAGE OF MASER DOWNTIME	17; 1.9%	14; 2.5%

Presented at 11th Annual
Precise Time and Time Interval
(PTTI) Applications and Planning
Meeting on 11-27-79

AT 14.6

HYDROGEN MASER IMPLEMENTATION IN THE DEEP SPACE NETWORK AT THE JET PROPULSION LABORATORY

Paul F. Kuhnle
Jet Propulsion Laboratory, Pasadena, California

ABSTRACT

Hydrogen masers (H-masers) are the most stable frequency standards in use today within the sampling intervals (τ) from 100 to 10^4 seconds. The Jet Propulsion Laboratory (JPL) employs hydrogen maser frequency standards in a variety of fixed and mobile applications, ranging from the 64-meter Deep Space Network stations to the 9-meter Astronomical Radio Interferometric Earth Surveying (ARIES) stations.

This paper describes the Frequency Standard Test Laboratory (FSTL) developed and implemented by JPL. This test laboratory has the capability to measure the frequency stability of five frequency standards including environmental parameters. Nine frequency standards may be evaluated simultaneously upon completion of the current instrumentation expansion program. Frequency stability measurements and environmental data on five H-masers are presented.

JPL is continuing hydrogen maser implementation plans by evaluating new H-maser designs for use during the 1980s.

INTRODUCTION

JPL supplies hydrogen masers as the prime frequency standard for navigation to the outer planets and for Very Long Baseline Interferometer (VLBI) experiments in both fixed and mobile ground stations. JPL has instrumented a Frequency Standard Test Laboratory to evaluate and test H-masers, other frequency standard types and reference frequency distribution equipment during development and prior to implementation in the user's facility. Selected representative test data recorded during the past two years is included in this report.

Hydrogen Masers at JPL

H-maser users at JPL have been using prototype and experimental H-masers for approximately 10 years for VLBI experiments and selected spacecraft tracking functions. In 1978, JPL formally installed one H-maser at each of the Deep Space Network (DSN) 64-meter tracking stations at Goldstone,

California and Madrid, Spain. A JPL DSN-type H-maser had previously been installed and has been in use at the DSN 64-meter tracking station near Canberra, Australia since 1976. In addition, JPL has operating H-masers at one DSN 26-meter tracking station at Goldstone, Owens Valley Radiometric Observatory (OVRO) and the ARIES mobile ground station. Three H-masers are retained at the JPL Pasadena complex. Two of these are reference masers in the test laboratory; the third is used as the DSN spare and by the ARIES geophysical mobile ground station.

Currently JPL has a total of eight H-masers in continuous use. These have been supplied by two well-known manufacturers and JPL. There are three Smithsonian Astrophysical Observatory (SAO) model VLG-10B H-masers which were supplied to JPL by the NASA Marshall Space Flight Center. The NASA Goddard Space Flight Center (GSFC) has loaned JPL one model NX H-maser and has, until recently, supplied JPL with three model NP H-masers.

JPL has three of the DSN type and one prototype H-maser in use at this time. Figure 1 tabulates the location, manufacturer, model and serial number of each H-maser in use by JPL today.

Some Selected Test Data Results to Date

JPL established a Frequency Standard Test Laboratory at the Pasadena, California complex and subsequently tested five H-masers between May 1978 and April 1979. These five are currently in use as shown in Figure 1. The units tested were JPL model DSN, serial numbers 2 and 3 and SAO model VLG-10B, serial numbers P5, P6, and P7.

The tests scheduled were considered to describe fully the necessary operating parameters of each H-maser. Additional parameters were usually recorded to assist in diagnostics or help explain the erroneous behavior of a desired parameter. The desired parameters recorded during these test programs were frequency stability versus sampling time (Allan variance) and frequency shift versus the environmental parameters of temperature, barometric pressure and the Earth's magnetic field.

Temperature tests were conducted on the five H-masers for step frequency shift in the temperature range of 21 to 29°C and then repeated from 29°C to 21°C. A step change in temperature usually causes the frequency to start shifting in less than one hour and it will continue to shift for approximately 40 hours with an exponential decay. The temperature coefficient for each H-maser tested is tabulated in Fig. 2. Of the environmental parameters, temperature presents the greatest frequency stability perturbation. It is not uncommon to experience room temperature fluctuations of 1 to 2°C in a diurnal or longer time period, resulting in a $1\text{-}2 \times 10^{-13}$ frequency shift. At the 64-meter tracking stations, the H-masers are in separate temperature-controlled rooms. These rooms are controlled to the nearest 0.1°C, thereby minimizing the

problem and reducing the temperature-dependent frequency shift to typically 1 x 10^{-14}.

Response to changes in the local barometric pressure was tested on the same H-masers. The test chamber pressure was increased by 6 inches of water and after approximately one hour decreased to minus 6 inches of water, relative to the starting ambient pressure. Because the frequency shift responses are instantaneous, the pressure differential must only be maintained long enough to determine the resultant frequency shift. The barometric pressure coefficient for the five H-masers is tabulated in Fig. 2. The resultant barometric pressure data shows that four of the five H-masers exhibit approximately the same frequency shift for an incremental pressure change. The exception is model VLG-10B Number P6 which exhibited an excessive frequency stability fluctuation during test. This H-maser at Goldstone has not always responded to storm barometric pressure fluctuations. It is planned to schedule a barometric pressure retest on this unit when sufficient H-masers are available to temporarily remove this unit from the field. A typical barometric pressure shift at Goldstone is approximately 0.3 inch Hg. The resultant frequency shift of the other four H-masers would be approximately 1 x 10^{-14}.

Frequency shift response to static magnetic field disturbances was measured on the five H-masers. The results are tabulated in Fig. 2. The resultant normalized frequency shift per gauss is 1 to 5 x 10^{-12} for four of the five H-masers. Magnetic field perturbations in the test laboratory are typically less than one milligauss under controlled operating conditions of minimal movement of ferrous materials. The measured magnetic field perturbations are typically five milligauss at the H-maser installation location within the 64-meter tracking stations. The resultant predicted frequency shift during these disturbances would be typically a maximum of 1 x 10^{-14}. The fifth unit (JPL-DSN2) was several times more sensitive to magnetic field than the other four H-masers tested. Following these tests, this H-maser was installed in a moly-permalloy magnetic shield box, which improved the shielding factor by a minimum of 100 or a predicted magnetic field coefficient of 1.4 x 10^{-13} per gauss.

A selected sample of Allan variance curves for four of the five H-masers tested since June 1978 is shown in Fig. 3.

The sampling times (τ) of less than approximately 1000 seconds are controlled by the signal-to-noise ratio. Each manufacturer designs H-masers to operate within a desired output power range. The JPL model DSN H-maser's nominal output power is approximately -87 to -89 dBm. The SAO model VLG-10B H-maser output power range is approximately -95 to -100 dBm. Therefore the data between the two SAO H-masers measured in June 1978 is approximately as expected. Later tests have used one SAO H-maser compared against one JPL H-maser.

Measurements at sampling times greater than 1000 seconds depict a degradation of frequency stability. This is due to "systematics," which is a combination of environmental effects and oscillator aging. In this set of specific cases, the curves peak at the sampling time of 20,000 seconds (approximately six hours), the 1/4 diurnal temperature cycle. Note that two of four curves exhibit this effect. The other conclusion is that all of these H-masers, except possibly SAO serial number P6, are aging. Since installation, P6 has been nearly continuously compared against a cesium beam frequency standard bank traceable to NBS. There is no indication versus this bank that this H-maser is aging. The curve between serial numbers P5 and P6 in June 1978 indicates that the aging is considerably less than all the other H-masers tested. JPL H-maser DSN-3 is not shown on this curve, but the approximate same slope is apparent as with all H-masers except P6. Note that the frequency stability curves exhibit a broad "bright line" (degradation hump) on two curves for sampling times between 100 and 800 seconds. This is caused by the cooling cycling rate of the building air conditioner. The lower dotted-line curve was recorded during November 1979 after the FSTL temperature control was improved. This is discussed later in this report.

Figure 4 again shows the Allan variance versus sampling time curve in Fig. 3. This plot has the measurement error bars and number of data samples available written beside each bar. In this case, where the number of samples is not shown, the number is greater than 51. Since all sampling times are simultaneously recorded, the number of samples increases as the sampling time decreases.

Frequency Standard Test Laboratory

A Frequency Standard Test Laboratory (FSTL) installation was initiated in August 1977 at the Pasadena complex to determine the operational performance of H-masers. An isolated building was obtained and is located at one end of the "Mesa" antenna range above and behind the Laboratory. This location was chosen because it is isolated from man-made disturbances of the Earth's magnetic field and has sufficient floor space for five H-masers and all instrumentation required at this time. Figure 5 is a view of this building with the Angeles National Forest in the background. The floor plan of this 700-square-foot building (Fig. 6) depicts the location of H-masers, environmental chamber and instrumentation. This laboratory is now equipped with instrumentation to simultaneously measure 12 channels of Allan variance and 12 continuous recording channels of long-term frequency shift.

Figure 7 is a block diagram of a single channel of this frequency stability measurement equipment. Figure 8 is a block diagram of the test configuration for comparing the frequency of three H-masers using three sets of the instrumentation shown in Fig. 7. Local barometric pressure, room and equipment temperature and Earth's magnetic field disturbances are continuously recorded as ancillary data to the frequency stability

measurements. Instrumentation is available to record frequency standard anomalies as required. Several examples are: vacion pump current, oven heater temperatures and cavity tuning bias voltage.

Figure 9 is a photograph of the instrumentation room, which contains nine electronic instrument cabinets. The equipment description is as follows, from left to right: (1) cabinets 1 and 2 are for environmental and anomaly measurements; (2) cabinet 3 is for general spectral and waveform analyses; cabinet 4 contains the RF reference isolation amplifiers, mixers and zero crossing detectors shown in Fig. 7; cabinets 5 through 8 each contain three channels of frequency stability measurement and recording equipment, and cabinet 9 contains general instrumentation, a rubidium frequency standard and two spare H-maser receiver crystal VCO's.

A combined temperature and barometric pressure chamber was designed and fabricated by JPL with non-magnetic materials to prevent distorting and attenuating the Earth's magnetic field around the H-maser. A separate connected heat exchanger preconditions the chamber air temperature for barometric pressure and temperature tests.

A 7-foot-diameter double axially concentric Helmholtz coil is used to generate static perturbations of the Earth's magnetic field. Generally, these coils are mounted around the environmental chamber to expedite the schedule on separately measuring H-maser frequency shift versus temperature and magnetic field. The environmental chamber and Helmholtz coil are shown in the far right corner of Fig. 10.

Standby AC power was installed to prevent power loss to the test laboratory. This equipment consists of a 4.5-kVA uninterruptible power supply (UPS) and a 30-kVA automatic starting generator. All frequency standards and critical instrumentation requiring power without interruption are connected to the UPS. The balance of the instrumentation, UPS input power and most of the air conditioning equipment is connected to the generator during primary power outages.

H-maser test results between May 1978 and April 1979 showed that both the laboratory temperature environment and instrumentation required improvement for future test programs to determine the prospective improved long-term frequency stability performance. These revisions are now completed. Subsequent tests show the new computer floor plenum air temperature to be stable to within 0.1°C peak to peak and the room 5 feet above the floor to 0.5°C peak to peak. The previous air conditioning system controlled the room from 1 to 3°C peak to peak for diurnal and longer time periods, depending on the outside weather conditions. An Allan variance test recorded during November 1979 showed considerable stability improvement using the same two H-masers previously recorded in April 1979. Compare the two curves dated April 1979 and November 1979 in Fig. 3. Note that at the Allan variance at 2×10^4 seconds sampling time

(τ) the "bright line" peak is not evident and the overall noise at sampling times greater than 1000 seconds is much lower. Room temperature control is considered to be the major factor in this improvement.

Additions and improvements to the instrumentation expanded the Allan variance and long-term frequency shift measurement capability to 12 channels. Additional recording instrumentation to continuously measure equipment temperature, magnetic field and room humidity has been added. This is sufficient instrumentation to simultaneously measure the stability of five H-masers as shown in Fig. 11.

Frequency shift versus barometric pressure increments have been difficult to measure in the past. It is expected that newer H-maser designs will exhibit even less barometric pressure sensitivity; therefore the environmental chamber has been strengthened to double the barometric pressure stimulus range to ±12 inches of water relative to the local barometric pressure.

It is intended to further improve the laboratory environment and instrumentation to meet the requirements from development and research of future frequency standards. Instrumentation improvements being considered and studied at this time are computerized automation of the data acquisition on a continuous basis, control of the test chamber humidity during environmental tests, and dual difference detection for frequency stability measurements of non-offsettable frequency standards.

Present Test Programs

JPL plans to continue use of the FSTL in the future to give frequency standard research and support to the JPL-operated Deep Space Tracking Station Network and other JPL-operated fixed and mobile ground stations.

An important task scheduled to start in December 1979 is the NASA-JPL program to evaluate the operating performance characteristics of two recently designed H-masers. These are the SAO Model VLG-11B and the GSFC Model NR.

Maintenance, repair and retest of all H-masers currently in field use by JPL is a continuing high priority project. The FSTL has done and will continue to do requalification after repair and diagnostics on non-obvious failures prior to repair. The FSTL has been and will continue to be scheduled to test other types of frequency standards (e.g., cesium beam), active reference frequency cable stabilizer equipment, frequency multipliers and synthesizers.

Recently the Laboratory scheduled and completed a series of tests on one superconducting cavity stable oscillator (SCSO) manufactured by Stanford University and purchased by Caltech. This was part of the JPL research program to evaluate new types of reference oscillators.

ACKNOWLEDGEMENTS

I wish to thank JPL engineers Albert Kirk and Roland E. Taylor for their participation in this program. Their task has been to operate the FSTL since inception. Both have been very involved in the recent upgrade of this laboratory and continued operation of the FSTL.

This paper presents the results of one phase of research carried out at the Jet Propulsion Laboratory, California Institute of Technology, under Contract No. NAS7-100, sponsored by the National Aeronautics and Space Administration.

LOCATION	MANUFACTURER	MODEL	SERIAL NUMBER
DSS 14 GOLDSTONE, CA	SAO	VLG 10 B	P6
DSS 63 MADRID, SPAIN	SAO	VLG 10 B	P7
DSS 43 CANBERRA, AUSTRALIA	JPL	DSN	1
DSS 13 GOLDSTONE, CA	JPL	PROTOTYPE	P2
OVRO BISHOP, CA	GSFC	NX	2
ARIES JPL	SAO	VLG 10 B	P5
FSTL, JPL	JPL	DSN	2
FSTL, JPL	JPL	DSN	3

MANUFACTURER CODE

GSFC: GODDARD SPACE FLIGHT CENTER

SAO: SMITHSONIAN ASTROPHYSICAL OBSERVATORY

JPL: JET PROPULSION LABORATORY

Fig. 1. JPL H-Maser Deployment

	VLG 10 B P5	VLG 10 B P5	VLG 10 B P6	VLG 10 B P7	DSN 3	DSN 2
TEMPERATURE $\frac{\Delta F}{F}$ /°C	-1.6×10^{-14}	-1.2×10^{-13}	-1.0×10^{-13}	7.0×10^{-14}	2.5×10^{-13}	-6.3×10^{-14}
BAROMETRIC PRESSURE $\frac{\Delta F}{F}$ / $"_{H_G}$	2.6×10^{-14}	2.6×10^{-14}	-3.4×10^{-13}	2.3×10^{-14}	-3.8×10^{-14}	-4.8×10^{-14}
MAGNETIC FIELD $\frac{\Delta F}{F}$ /GAUSS	1.6×16^{-12}	3.0×10^{-12}	5.0×10^{-12}	2.8×10^{-12}	4.8×10^{-12}	1.4×10^{-11}

Fig. 2. H-Maser Environmental Parameters

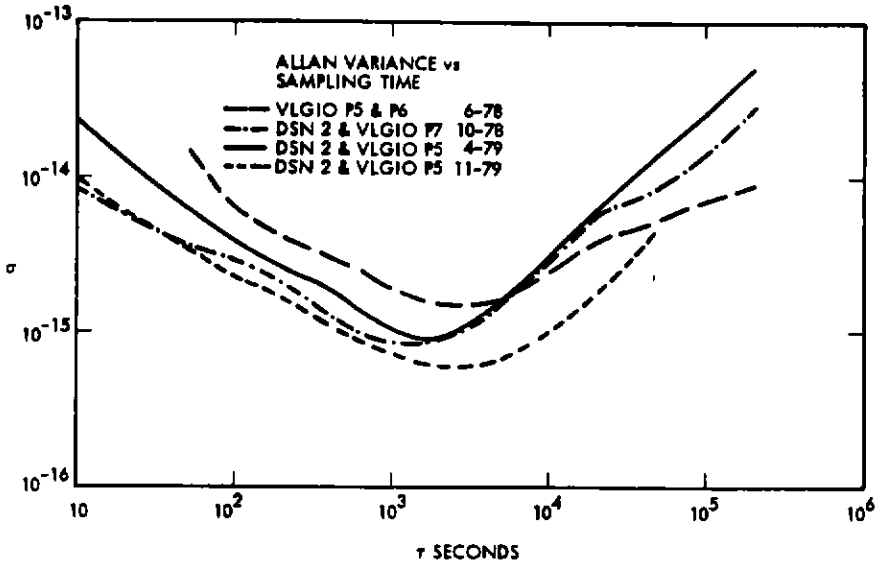

Fig. 3. Allan Variance vs. Sampling Time

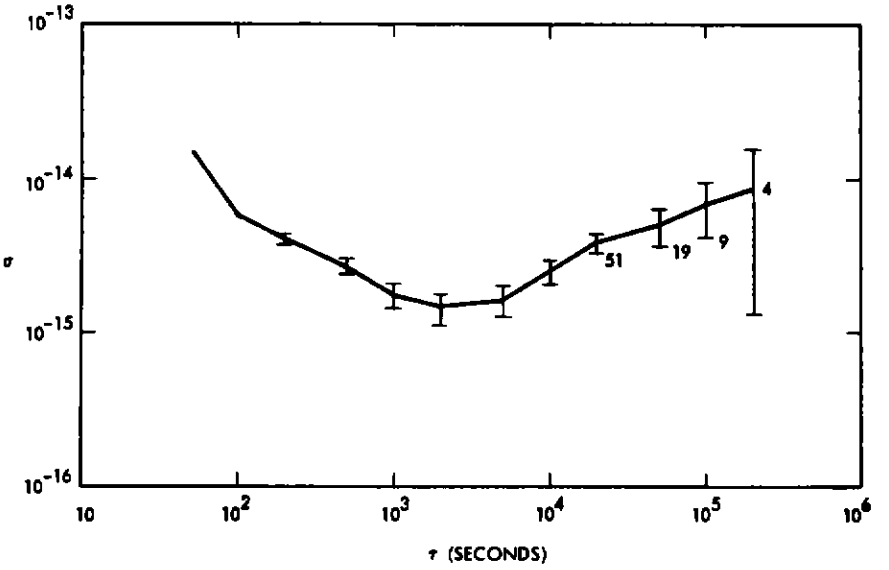

Fig. 4. Allan Variance vs. Sampling Time, with Error Bars

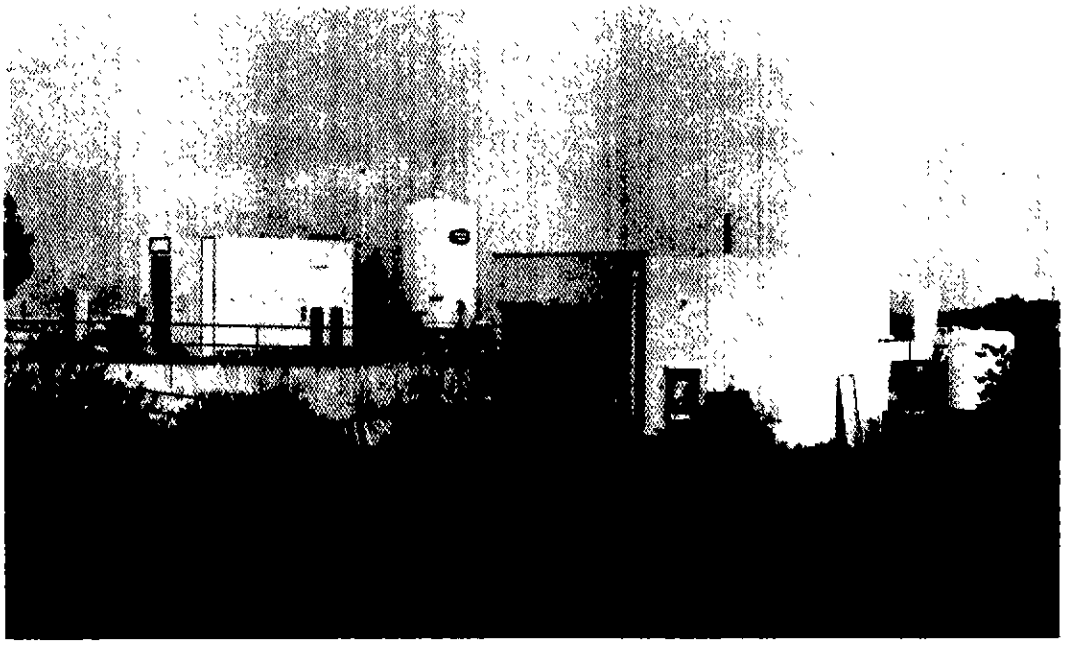

Fig. 5. JPL Frequency Standard Test Laboratory

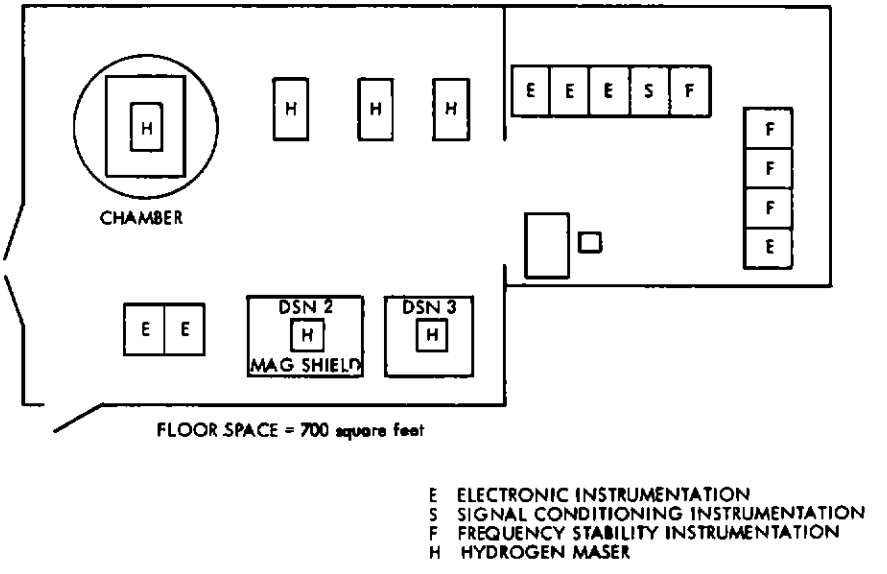

Fig. 6. Frequency Standard Test Laboratory Floor Plan

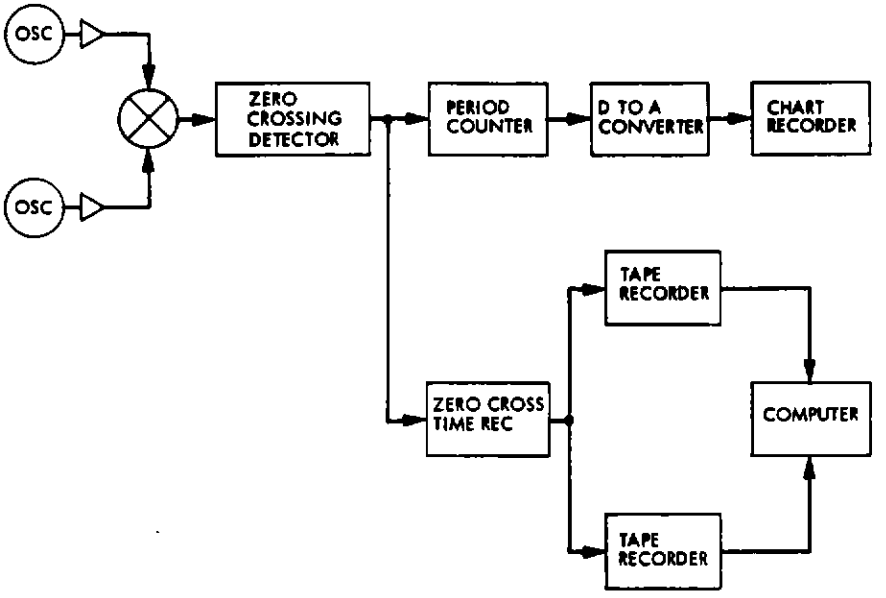

Fig. 7. Frequency Stability Instrumentation Block Diagram

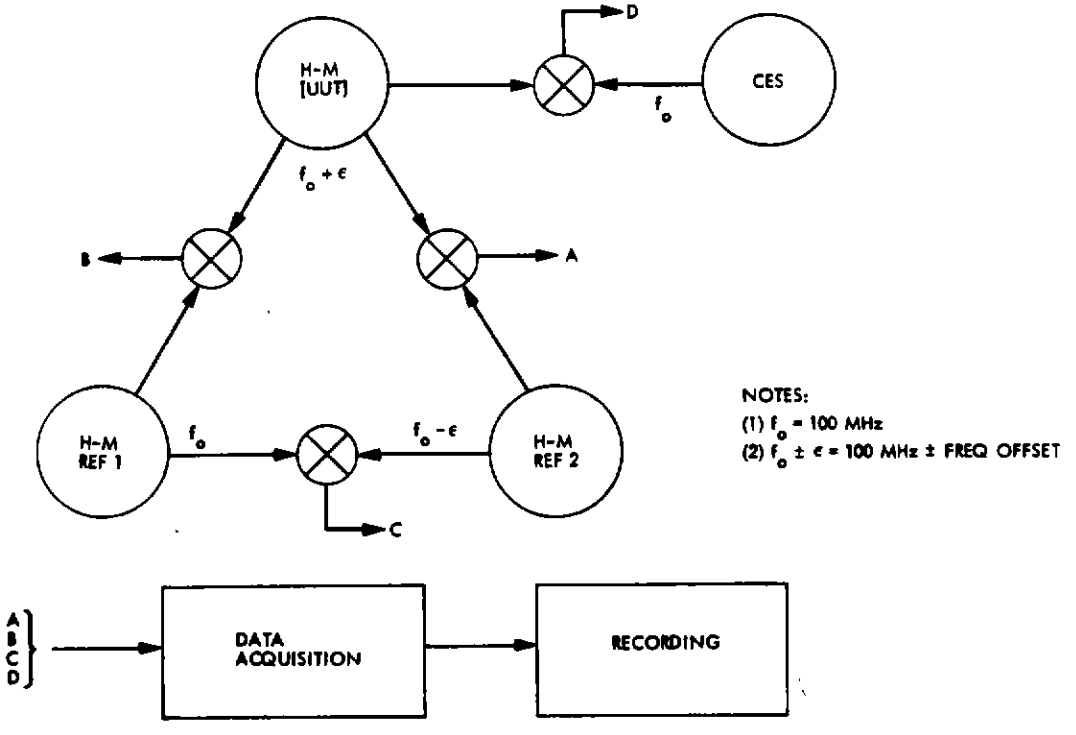

Fig. 8. Test Configuration for Stability Comparison of Three H-Masers

Fig. 9. Instrumentation Room Containing All Measurement Instrumentation

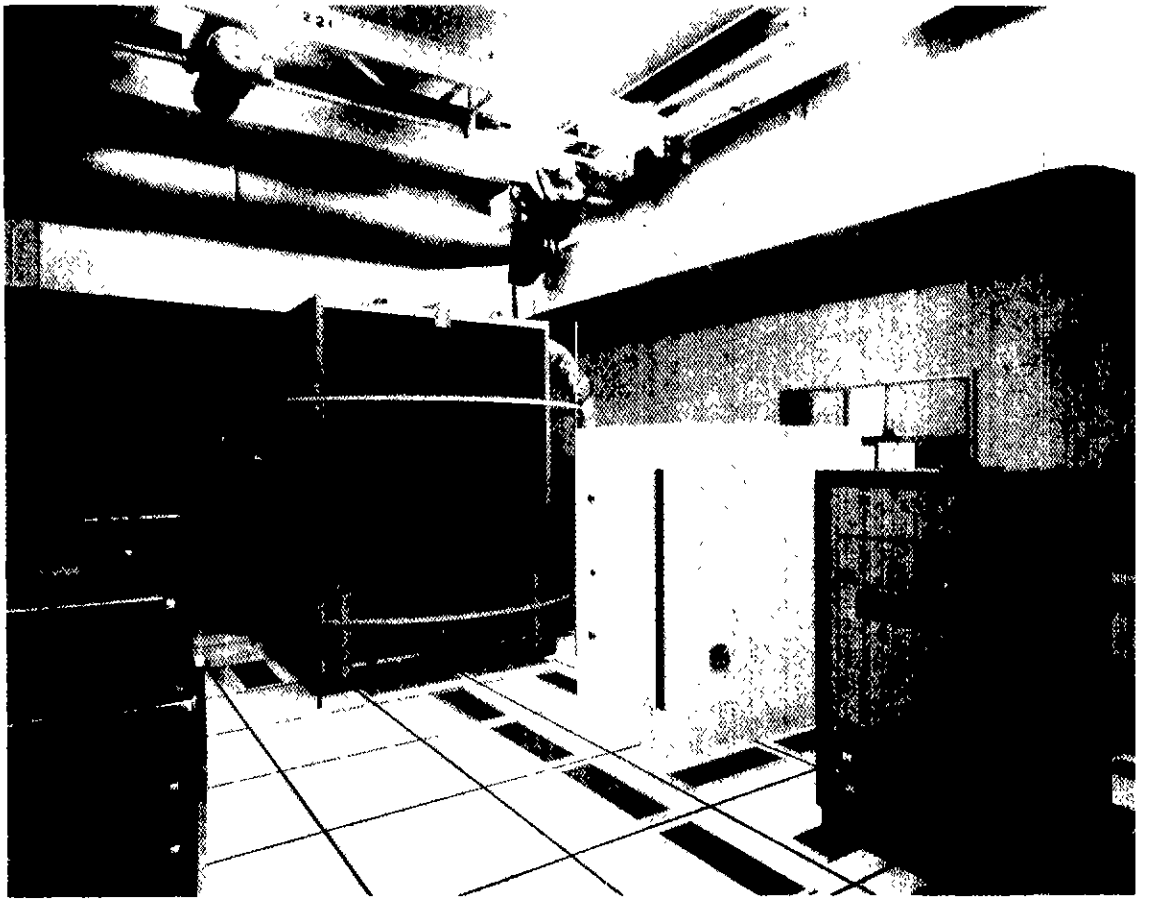

Fig. 10. Frequency Standard Room with Space on Right Side for H-Masers in Test and Environmental Chamber at Far Right

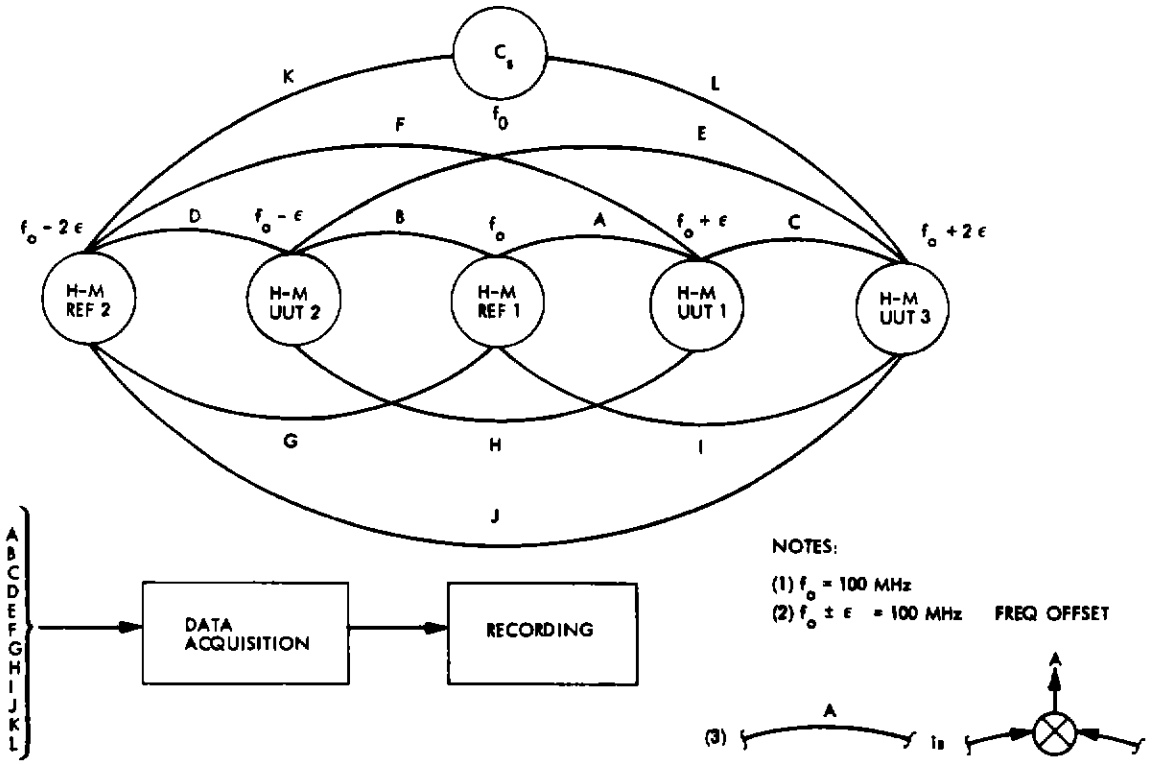

Fig. 11. Test Configuration for Stability Comparison of Five H-Masers